

E²MPL: An Enduring and Efficient Meta Prompt Learning Framework for Few-shot Unsupervised Domain Adaptation

Wanqi Yang, Haoran Wang, Lei Wang, Ge Song, Ming Yang, Yang Gao

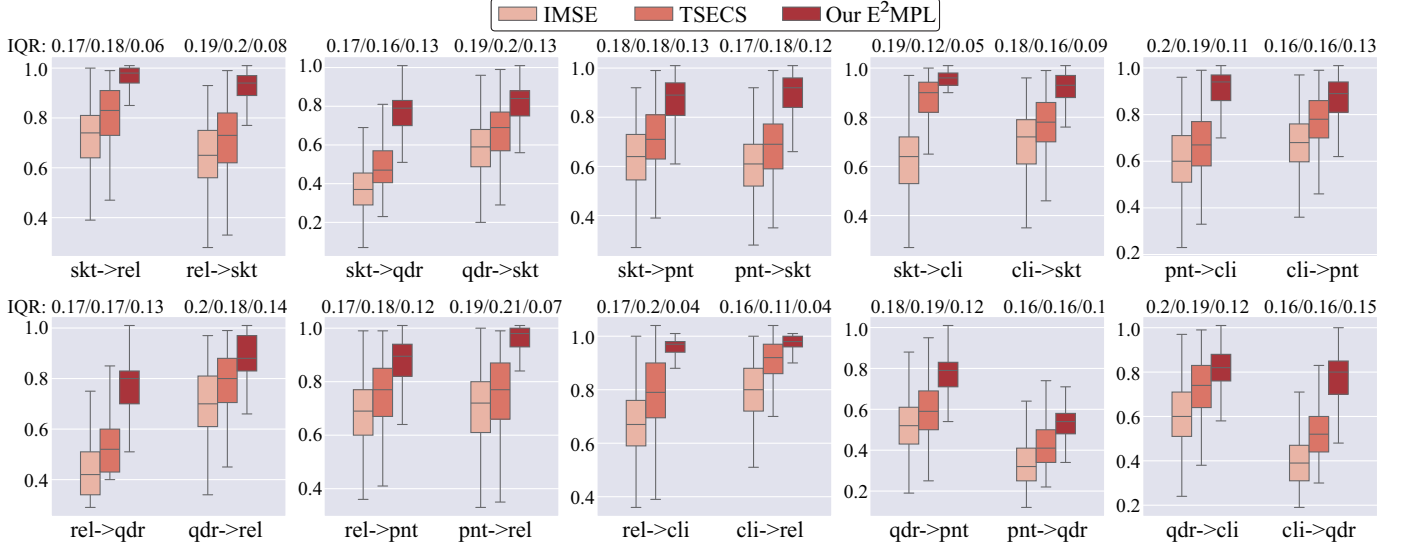


Fig. 1: Illustration of the accuracy boxplot and Interquartile range (IQR) of three FS-UDA models that adapt to 3600 test tasks with 5-way 1-shot setting. It is observed that our E²MPL exhibits much more enduring and effective performance across diverse tasks in *DomainNet* dataset.

Abstract—Few-shot unsupervised domain adaptation (FS-UDA) leverages a limited amount of labeled data from a source domain to enable accurate classification in an unlabeled target domain. Despite recent advancements, current approaches of FS-UDA continue to confront a major challenge: models often demonstrate instability when adapted to new FS-UDA tasks and necessitate considerable time investment. To address these challenges, we put forward a novel framework called Enduring and Efficient Meta-Prompt Learning (E²MPL) for FS-UDA. Within this framework, we utilize the pre-trained CLIP model as the backbone of feature learning. Firstly, we design domain-shared prompts, consisting of virtual tokens, which primarily capture meta-knowledge from a wide range of meta-tasks to mitigate the domain gaps. Secondly, we develop a task prompt learning network that adaptively learns task-specific prompts with the goal of achieving fast and stable task generalization. Thirdly, we formulate the meta-prompt learning process as a bilevel optimization problem, consisting of (outer) meta-prompt learner and (inner) task-specific classifier and domain adapter. Also, the inner objective of each meta-task has the closed-form solution, which enables efficient prompt learning and adaptation to new tasks in a single step. Extensive experimental studies demonstrate the promising performance of our framework in a domain adaptation benchmark dataset *DomainNet*. Compared

with state-of-the-art methods, our method has improved accuracy by at least 15.4% and reduced the time by 68.5% on average in 5-way 1-shot tasks, and improved accuracy by 8.7% and reduced the time by 74.1% on average in 5-way 5-shot tasks. Moreover, our approach exhibits more enduring performance than the other methods, *i.e.*, being more stable across 3600 test tasks.

Index Terms—Few-shot unsupervised domain adaptation, Meta learning, Meta prompt learning, Bilevel optimization

I. INTRODUCTION

In unsupervised domain adaptation (UDA), when the labeling cost is high or the access to labeled data is limited, it cannot be guaranteed that sufficient labeled data will be available for each category in the source domain. This limitation can severely impair the domain adaptation capabilities and consequently degrade the classification performance in the target domain. To address these issues, a setting known as few-shot unsupervised domain adaptation (FS-UDA) [1] [2] [3] has emerged, which only leverages few-shot labeled data in the source domain for UDA, offering a potentially viable solution. An FS-UDA model is expected to acquire general knowledge from base classes during training and subsequently guide the classification of novel classes during testing. However, both insufficient labeled data in the source domain and large domain shifts between the source and target domains make FS-UDA a particularly challenging task.

Previous FS-UDA methods have addressed domain shifts primarily through the development of cross-domain similarity

Wanqi Yang, Haoran Wang, Ge Song and Ming Yang are with the School of Computer Science and Technology, and also with Ministry of Education Key Laboratory of NSLSCS, Nanjing Normal University, Nanjing, China. (e-mail: yangwq@njjnu.edu.cn, myang@njjnu.edu.cn).

Lei Wang is with the School of Computing and Information Technology, University of Wollongong, Australia. (e-mail: leiw@uow.edu.au).

Yang Gao is with the Department of Computer Science and Technology, Nanjing University, Nanjing, China. (e-mail: gaoy@nju.edu.cn).

metrics [1], the extraction of high-level semantic features across domains [3], or the incorporation of domain adversarial loss into the meta-learning framework [2]. However, we observed that these approaches show performance instability when adapting to various new tasks. As illustrated in Fig. 1, compared to our E²MPL, the accuracy boxplots of previous methods (IMSE [1] and TSECS [3]), tested on 3600 distinct tasks, perform more dispersed with a lower median and a higher Interquartile range (IQR) ¹.

We believe that a promising FS-UDA model should be able to i) generalize effectively and stably to new and unseen tasks, and ii) ensure that the learning process is computationally efficient while maintaining high performance.

To achieve this goal, we employ the pre-trained CLIP as the backbone of our model and introduce learnable virtual prompts as the inputs to CLIP for a lightweight yet promising update, enabling rapid adaptation to downstream various tasks without necessitating full parameter updates of CLIP. However, conventional visual prompt learning methods [4] [5] can easily overfit a limited number of training samples, as well as hardly address the domain shift. This could hinder the generalizability of the CLIP models for FS-UDA tasks. In light of the generalizability challenges faced by prompt learning, meta-prompt learning emerges as a viable alternative. Several meta prompt learning methods [6] [7] [8] leverage the meta learning strategy to learn the general prompts. For instance, DAM-VP [6] introduces a specific meta-prompt vector for each data subset, tailored to visual differences to mitigate the variations of data distribution within the same dataset, but it is not suitable for substantial discrepancy between domains. Prompt Meta-Regularization (ProMetaR) [8] was proposed to employ meta-regularization to alleviate overfitting, but it is limited by its reliance on text prompts and learning prompts is relatively time-consuming, requiring multiple updates for each task. Consequently, there is an urgent need to develop a more effective and efficient meta-prompt learning framework specifically designed for FS-UDA tasks.

To facilitate domain adaptation and task generalization, we design domain-shared prompts and task-specific prompts. Specifically, we embed domain-shared prompts into the feature embedding module to learn the general features across domains. To better adapt CLIP to various tasks, we make additional use of the pre-trained prompt network to generate task-specific prompts, which not only mitigates domain gaps but also helps the model focus on crucial information for the current task, resulting in improved stability.

Therefore, we propose a novel Enduring and Efficient Meta-Prompt Learning Framework for FS-UDA, namely E²MPL. Formally, the proposed meta-prompt learning process is formulated as a bilevel optimization problem consisting of the (outer) meta-prompt learner and the (inner) base learner [9]. We design the meta-prompt learner over the collection of meta-tasks to obtain the domain-shared prompts and task-specific prompts aforementioned. Meanwhile, we build two

base learners (*i.e.*, a classifier and a domain adapter) for each of these meta-tasks, respectively. The classifier learns the optimal classification parameter for this task, while the domain adapter learns the optimal projection parameter to transform the target domain data close to the source domain data. To make the proposed meta-prompt learning process computationally efficient, instead of the time-consuming iterative calculation, both the classifier and the adapter enjoy a globally optimal closed-form solution that can be calculated in one step within each task. Thus, our E²MPL can efficiently adapt the model to new tasks. Our main contributions can be summarized as follows.

- 1) **A novel meta-prompt learning framework E²MPL for FS-UDA.** We propose a bilevel optimization meta-prompt learning framework, where the outer meta-prompt learner captures meta-prompts from meta-tasks and the inner classifier and domain adapter are designed for each task with closed-form solutions, enabling efficient and stable adaptation to new tasks.
- 2) **Domain-shared and task-specific prompts.** Leveraging CLIP’s pretrained vision backbone, we introduce domain-shared and task-specific prompts optimized through meta-learning, which collaboratively enhance cross-domain alignment while preserving task-specific discriminability.
- 3) **Enduring and efficient performance.** Extensive experiments on *DomainNet* validate our EMPL achieves more effective and enduring performance across diverse tasks, and takes significantly less time to adapt to new tasks, compared to the alternative.

II. RELATED WORK

A. Unsupervised Domain Adaptation

The UDA setting aims to reduce the domain gap and leverage sufficient data from the labeled source domain to achieve classification in the unlabeled target domain. Many UDA methods [10]–[12] are based on the maximum mean discrepancy to minimize the difference in features between domains. By constructing deep networks, several methods [13]–[15] have learned the domain-invariant representation, which is transferable between different domains. Long *et al.* [11] introduced multiple domain adaptation modules in the high layers of deep convolutional network to match the mean embeddings of the distributions according to the maximum mean discrepancy criterion. Subsequently, they [14] proposed a joint maximum mean discrepancy criterion to align the distributions of multiple domain-specific fully connected layers. Roy *et al.* [16] developed a unified deep domain adaptation framework and built domain alignment layers to match the feature distributions between different domains. If there are pseudo-labels with high confidence, UDA is converted to SSDA, which is beneficial for semi-supervised learning effects. By applying a gradient-variance-based selection mechanism, Yang *et al.* [17] exploits a friendly subset instead of the entire open-set dataset to enhance the ID classification capacity of the model, which can be applied to the SSDA problem.

¹A box plot is a method for demonstrating graphically the locality, spread and skewness groups of numerical data through their quartiles, where Median (Q2) is the middle value, and Interquartile range (IQR) is the distance between the upper and lower quartiles, *i.e.*, $IQR=Q3-Q1$, for statistical dispersion.

Moreover, adversarial training is widely used to tackle domain shifts. There are several methods [18]–[20] that developed domain-invariant feature generators and a domain discriminator to distinguish their authenticity/fakeness. DANN [18] learned domain-invariant features by training a domain classifier with a gradient reversal layer. ADDA [19] provided a generalized framework to combine adversarial learning, discriminative feature learning, and untied weight sharing. CDAN [21] used discriminative classification predictions to align the domains. MCD [12] maximized the discrepancy between task-specific classifiers to perform adversarial learning with the feature generator. To learn domain-invariant and semantic representations, a graph convolutional adversarial network [22] was built to jointly perform the alignment of the data structure, domain and class centroid. In addition, contrast learning is also commonly used in UDA. CPRC [23] generates captions directly from images using the automatically learned cross-modal generator. For an unseen class from the UDA setting, CRV [24] holds a realistic setting that unlabeled data may come from unseen classes in the labeled set. CKGE [25] provides explainable recommendations with the consideration of different learning motivations from talents. In sum, existing UDA methods achieved domain adaptation with sufficient labeled source domain data. However, they would not work when encountering the issues of scarce labeled source domain and task-level generalization that exist in our FS-UDA setting.

B. Prompt Learning for Computer Vision

Currently, prompt learning has recently been integrated into the field of computer vision. The primary objective of prompt learning is to utilize pre-trained models to offer valuable insights for downstream tasks through visual prompts. Concretely, learning methods for single-modal visual prompt learning include concatenating optimizable vector sequences [4] [26] [27] [28], adding pixel-level optimizable disturbance [29]–[31], learning prompt network layer [32]–[34], component-oriented combinatorial prompt learning [6], network structure search [36], *etc.* Concatenated optimizable vector sequences based on the Transformer structure are generated by concatenating additional optimizable vector sequences, such as VPT [4], on top of the original input sequence or each layer feature sequence of the Transformer structure. The inclusion of pixel level optimization allows for the disturbance independent of the model structure, enabling direct addition of an optimized random disturbance block or a rectangular box to the pixel space of the input image, such as VP [29]. The learning prompt network layer serves as a plug-in prompt module added primarily between the backbone network layers or as a generative prompt module outside the backbone network, such as Pro-Tuning [32], PGN [33]. Composition prompt learning for specific components involves designing different prompt templates for various data categories, such as DAM-VP [6]. The network structure search involves selecting a parameter-effective method at random for different downstream datasets to tune and then choosing the best performing one as the final prompt on that dataset. For example, NOAH [36] integrates the adapter [37], LoRA [38], and VPT [4] as a splicable prompt module.

There are also multimodal prompt learning methods. CoOp [39] enhances the classification of few-shot images by optimizing continuous prompts to fine-tune CLIP. CoCoOp [40] proposes learning conditional prompts based on image features to further improve the generalization of CoOp. Moreover, APLeNet [41] argues that the potential of Visual Language Model in remote sensing generalization task has not been fully realized; it introduces an attention-driven injection module to generate visual tokens from visual content features and style properties. Additionally, AD-CLIP [5] argues that the aforementioned methods fail to take domain gaps into account. Therefore, it conditions prompt learning of both image style and content features simultaneously in order to acquire domain-invariant and class-generalizable knowledge. ProD [28] utilized the prompting mechanism in the transformer to disentangle the domain-general and domain-specific knowledge from the backbone features for cross-domain few-shot image classification. However, these methods for prompting on text encoders are usually limited by text input. In our work, we need useful prompts to deal with domain gap and task generalization, as well as an efficient prompt learning method.

C. Meta-Learning for Few-shot Learning

In few-shot learning (FSL), it is key to leverage auxiliary data to train a generalizable model to prevent overfitting, even if only a few samples per category are available for the current task. In recent years, common few-shot learning methods can be mainly divided into two aspects: meta-learning optimization-based methods and metric-based methods.

Meta-learning optimization-based methods [42], [43] typically involve training a meta-learner on a collection of meta-tasks to learn general model parameters, *i.e.*, initializing the parameters and hyper-parameters that can adapt to new tasks. For example, MAML [43] and Meta-SGD [44] learned a well-initialized model that updated the direction and learning rate, respectively. LEO [45] extended MAML to learn a latent representation space. In addition, Franceschi *et al.* formulated meta-learning through bilevel optimization [9], while Qin *et al.* proposed the concept of intra-domain and inter-domain meta-knowledge [46], which also inspired us.

On the other hand, metric-based methods [47]–[49] focus on learning a general feature metric space through episodic training on the auxiliary dataset [50]. Classically, ProtoNet [47] learns the class prototypes in the support set and then classifies the query samples according to their maximum similarity to these prototypes. Li *et al.* meanwhile leveraged the covariance matrix [48] and local descriptors [51] for the measurement of image to class. Note that in the above methods, the support and query sets in an FSL task are usually in the same domain. They are not capable enough to handle the domain gap between the support set in source domain and the query set in target domain that exists in our FS-UDA setting.

III. METHODOLOGY

In this section, we begin by presenting the definition of FS-UDA problem. Next, we detail the design of our prompt module. Subsequently, we introduce our meta-prompt learning

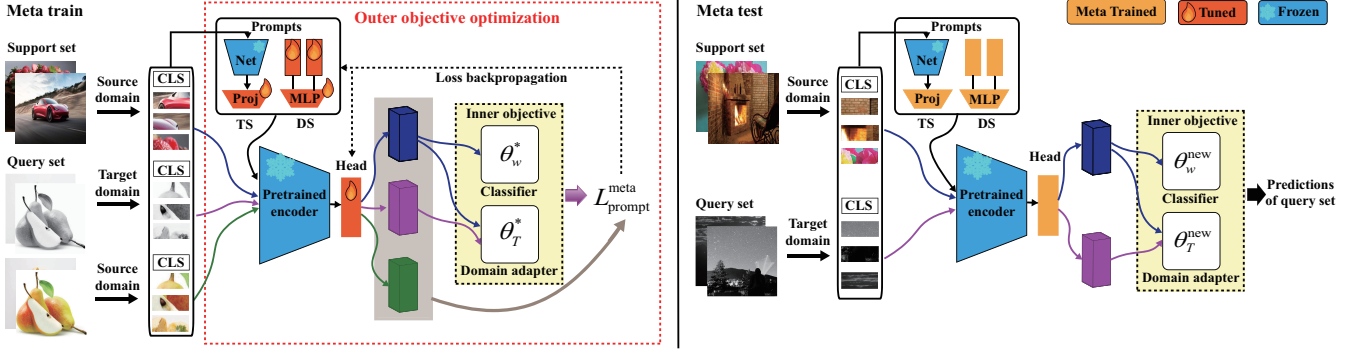


Fig. 2: Illustration of the proposed E²MPL for FS-UDA. For each meta task, the support set, query set, domain-shared prompt (DS), and task-specific prompt (TS) are first fed to the pre-trained CLIP image encoder and head layer to train a classifier and a domain adapter to get the optimal parameters θ_ω^* and θ_T^* , respectively. Then, the query set from both source and target domains is used to calculate the meta-train loss, including the source domain classification loss $\mathcal{L}_c^{\text{meta}}$, target domain entropy minimum loss $\mathcal{L}_d^{\text{meta}}$, and class discrimination loss $\mathcal{L}_f^{\text{meta}}$. Finally, these losses are back-propagated to update the prompt module and head layer. The above process is conducted repeatedly over all meta tasks. For a test task, the support set is fed to the trained model to get the optimal $\theta_\omega^{\text{new}}$ and θ_T^{new} for final prediction in the query set.

framework grounded in bilevel optimization [9]. Lastly, we detail the implementation of the classifier and domain adapter, respectively.

A. Problem Definition

A N -way, K -shot UDA task. The FS-UDA setting involves two domains in total: a source domain \mathcal{S} and a target domain \mathcal{T} , both of which are shared by all tasks. A N -way, K -shot UDA task consists of a support set D_S^{sup} derived from \mathcal{S} and a query set D_T^{que} derived from \mathcal{T} . The support set D_S^{sup} comprises N classes with K samples per class from the source domain. Meanwhile, the query set D_T^{que} contains $N \times N_q$ target domain samples from the same set of N classes as the support set. Our goal is to train a general model capable of quickly generalizing to new tasks, accurately classifying the query set D_T^{que} given the few-shot support set D_S^{sup} of the new task. Note that the classes in the meta-testing tasks are not observed during the meta-training, ensuring that the model could generalize to previously unseen classes during the meta-testing.

Model architecture. Our framework mainly consists of a pre-trained CLIP image encoder f_e , a head layer h_v , a task-specific classifier, a task-specific adapter and a learnable prompt module. The pre-trained CLIP encoder is frozen during training, and the classifier and adapter can directly calculate their parameters without optimization; Thus, only the prompt module and head layer need to be optimized.

The flowchart of our framework. Figure 2 illustrates the meta-train and meta-test process of our E²MPL. During the meta-train phase, in each episode, we construct a support set D_S^{sup} from the source domain, a query set D_T^{que} from the target domain, as well as an additional query set D_S^{que} from source domain for classifier training. For each meta-task, the support set, query set, domain-shared prompts and task-specific prompts are first passed through the pre-trained encoder and the head layer to obtain the features of the current task, and then sent to the classifier and domain adapter to calculate their optimal parameters θ_ω^* and θ_T^* , respectively. Afterwards, the query set (D_S^{que} and D_T^{que}) is used to calculate the meta-prompt loss (i.e., classification loss $\mathcal{L}_c^{\text{meta}}$, entropy

minimum loss $\mathcal{L}_d^{\text{meta}}$, and class discrimination loss $\mathcal{L}_f^{\text{meta}}$) among the meta-train tasks. Finally, the meta-prompt loss is backpropagated to optimize the prompt parameters and the head-layer parameter. During the meta-test phase, these prompt parameters are not updated. For each test task, the support and query sets are fed into the classifier and adapter to calculate their optimal parameters $\theta_\omega^{\text{new}}$ and θ_T^{new} . Based on these parameters, the query set from the target domain is projected into the source domain space for the final prediction. Finally, we calculate the average classification accuracy of different test tasks for performance evaluation.

B. Meta-Prompt Design

In the setting of FS-UDA, it is not feasible to train a model with a large number of parameters relying solely on a small number of data samples. Therefore, we employ the pre-trained CLIP as the backbone and introduce meta-prompt learning for a lightweight update. Meta-prompt learning enables the model to acquire meta-knowledge from multiple meta-tasks, which can achieve the domain adaptation and task generalization. To this end, we design domain-shared and task-specific prompts.

Domain-shared prompts. Existing prompt learning methods usually align the prompts between the source and target domains or the image and text prompts to mitigate domain gaps [5], but they require a large amount of data support to enhance the effectiveness of domain alignment. In light of this issue and inspired by VPT [4], we design domain-shared prompt tokens between the source and target domains that are concatenated by feature embedding for model training. This approach encourages the model to learn similar feature representations between the source and target domains to reduce the domain gap.

Task-specific prompts. Existing pre-trained models (such as CLIP) usually have poor generalization ability for unseen classes after prompt tuning, since they suffer from overfitting to the training classes [40]. Drawing inspiration from PGN [33] and aiming to better adapt the model to new classes, we introduce prior knowledge by utilizing a pre-trained prompt network that is frozen to preserve the class generalization of

the model. The prompt network can generate input-dependent prompts for the current task, allowing each image to receive specific prompts instead of using a fixed set of prompts, enabling the model to quickly adapt to unseen classes.

Specifically, the design approach for inputting domain-shared prompts and task-specific prompts together with image tokens into CLIP is illustrated in Fig. 2. Let P_c represent domain-shared prompts, P_k represent task-specific prompts from pre-trained prompt network, e_0 is the embedding of an additional learnable classification token ([CLS]), and \mathcal{E} is a sequence of embedding image patches. The input to CLIP can be written as

$$x = [e_0, f_1(P_c), f_2(P_k), \mathcal{E}], \quad (1)$$

where $[\cdot, \cdot]$ represents the concatenation operation, and both f_1 and f_2 represent mapping functions implemented through MLP are used to embed prompt tokens.

In the downstream tasks, as shown in Fig.2, the entire CLIP network is frozen, and the prompt parameters (including learnable domain-shared prompt tokens P_c , and its following MLP parameters θ_m , the projection parameter θ_p of task-specific prompts P_k , and the head parameters θ_h) are optimized, which are denoted as $\Theta = (P_c, \theta_m, \theta_p, \theta_h)$ in the following for clarity. Then, the prompt parameters Θ can be solved by

$$\Theta^* = \arg \min_{\Theta} \mathcal{L}(D_S, D_T), \quad (2)$$

where \mathcal{L} is the meta-prompt loss function, D_S and D_T represent data sets for the source and target domains, respectively.

In the following, our primary task is to learn the prompt parameters Θ in an efficient way. In summary, we design a meta prompt learning framework in the meta-training phase, which will be introduced in Section III-C. Then, in the meta-test phase, the learned prompt parameters along with the task-specific data are utilized as a new input for accurate classification in new tasks.

C. Proposed Meta Prompt Learning Framework

We now develop a meta prompt learning framework, E²MPL, to learn domain-shared prompts and task-specific prompts from meta-tasks such that the model can adapt to new tasks. Specifically, the learning process can be formulated as a bilevel optimization problem, where the inner objective is conducted on the support set to learn a classifier and a domain adapter that handle the current task, while the outer objective is conducted on the query set to update the prompt parameters for storing the corresponding meta-knowledge.

(1) For the inner objective:

For each meta task i , with the prompt parameters fixed, we design the two base learners (\mathcal{A} for classification and \mathcal{B} for domain alignment) to calculate their optimal parameters θ_ω^* and θ_T^* , respectively. This efficiency makes it possible to quickly obtain classifiers in few-shot learning scenarios without complex iterative optimization processes. Let $Z_{S,i}^{\text{sup}}$ and $Z_{T,i}^{\text{que}}$ represent the feature embeddings that are used for

classification and domain adapter. Then, the inner objective functions can be written by:

$$\begin{aligned} \theta_\omega^* &= \arg \min_{\theta_\omega} \mathcal{A}(D_i^{\text{sup}}; \theta_\omega) \\ &= \arg \min_{\theta_\omega} \mathcal{L}_c^{\text{base}}(Z_{S,i}^{\text{sup}}, Y_{S,i}^{\text{sup}}; \theta_\omega), \end{aligned} \quad (3)$$

$$\begin{aligned} \theta_T^* &= \arg \min_{\theta_T} \mathcal{B}(D_i^{\text{sup}}, D_i^{\text{que}}; \theta_T) \\ &= \arg \min_{\theta_T} \mathcal{L}_d^{\text{base}}(Z_{S,i}^{\text{sup}}, Z_{T,i}^{\text{que}}; \theta_T). \end{aligned} \quad (4)$$

Here, $\mathcal{L}_c^{\text{base}}(\cdot)$ and $\mathcal{L}_d^{\text{base}}(\cdot)$ represent the loss functions of classification and domain alignment, which will be described in Sections III-D and III-E, respectively.

(2) For the outer objective:

After obtaining the (inner) optimal θ_ω^* and θ_T^* for each meta task i , we update the prompt parameters Θ by minimizing the meta prompt loss, which consists of the classification loss $\mathcal{L}_c^{\text{meta}}$, the entropy minimization loss $\mathcal{L}_d^{\text{meta}}$, and the class discrimination loss $\mathcal{L}_f^{\text{meta}}$. Specifically, the classification loss $\mathcal{L}_c^{\text{meta}}$ is calculated by using θ_ω^* to classify the query set D_i^{que} from the source domain. Furthermore, due to the domain gap between the target and source domain data, we use θ_T^* to project the target domain data into the feature space close to the source domain data. Then, the entropy minimization loss $\mathcal{L}_d^{\text{meta}}$ is calculated for the projected target domain data.

In addition, we also design a class discrimination loss $\mathcal{L}_f^{\text{meta}}$, which minimizes the intra-class scatter matrix S_w and maximizes the inter-class scatter matrix S_b to bring the same-class samples closer together while pushing those of different classes farther apart, thereby improving the classification performance, which can be written by:

$$\mathcal{L}_f^{\text{meta}} = S_w - \lambda_s S_b, \quad (5)$$

where λ_s is a learnable hyperparameter. Since the target domain data are unlabeled, we use the cosine similarity between the target domain query samples and the source domain support samples to define the "same-class" samples. If the similarity is greater than a certain threshold, it is considered to be of the same class; otherwise, it is considered different. The threshold is automatically learned by the model (usually in the range of 0.65-0.8).

Formally, the losses will be back-propagated to update the prompt parameters Θ . Thus, the outer objective function can be written by:

$$\begin{aligned} \min_{\Theta} & \mathcal{L}_c^{\text{meta}}(D_i^{\text{que}}; \Theta, \theta_\omega^*) + \lambda_d \mathcal{L}_d^{\text{meta}}(D_i^{\text{que}}; \Theta, \theta_T^*) \\ & + \lambda_f \mathcal{L}_f^{\text{meta}}(D_i^{\text{que}}; \Theta, \theta_\omega^*, \theta_T^*), \end{aligned} \quad (6)$$

with $\theta_\omega^* = \mathcal{A}(D_i^{\text{sup}}; \Theta)$
and $\theta_T^* = \mathcal{B}(D_i^{\text{sup}}, D_i^{\text{que}}; \Theta)$,

where λ_d and λ_f are hyperparameters that regulate the balance between the losses. The optimal task-specific parameters θ_ω^* and θ_T^* obtained in the inner objective are used for classification and domain alignment in the query set, respectively.

Accordingly, the prompt parameters Θ in the outer objective will be iteratively updated in multiple meta-tasks to acquire meta-knowledge for rapid adaptation to new tasks.

D. Ridge Regression for Classification

Traditional meta-learning often involves multiple optimizations in the inner loop to update parameters, which is time-consuming and poses a significant challenge for quickly and effectively adapting to new classes. Ridge regression, with its closed-form solution, regularization, differentiability, and computational efficiency, becomes a good choice for efficiently adapting to new classes in few-shot learning. For computational efficiency and inspired by recent work [52], we use ridge regression to construct the base learners for each meta task. The optimal parameters θ_ω^* can be directly calculated as

$$\begin{aligned} \theta_\omega^* &= \arg \min_{\theta_\omega} \left\| Z_{S,i}^{\text{sup}} \theta_\omega - Y_{S,i}^{\text{sup}} \right\|^2 + \gamma_\omega \|\theta_\omega\|^2 \\ &= \left(Z_{S,i}^{\text{sup} \top} Z_{S,i}^{\text{sup}} + \gamma_\omega I \right)^{-1} Z_{S,i}^{\text{sup} \top} Y_{S,i}^{\text{sup}}, \end{aligned} \quad (7)$$

where γ_ω is a learnable regularization parameter. The above matrix to inverse are in $m \times m$ (m is the dimensionality of feature embeddings). To improve computational efficiency and reduce memory requirements, we use the Woodbury identity [53] to reformulate the above equation as

$$\theta_\omega^* = Z_{S,i}^{\text{sup} \top} \left(Z_{S,i}^{\text{sup}} Z_{S,i}^{\text{sup} \top} + \gamma_\omega I \right)^{-1} Y_{S,i}^{\text{sup}}, \quad (8)$$

where the matrix to inverse reduces to $n \times n$ (n is the number of support samples in a task). Because n is much less than m in the FS-UDA setting, θ_ω^* can be efficiently calculated.

E. Cross-domain Projection for Domain Adaptation

As the query set and the support set come from different domains, we design a domain adapter to align the domains in each meta task. Typically, domain adapters introduce a learnable transformation layer that effectively adjusts the feature distribution between the two domains [54]. Since the target domain data are not labeled, direct cross-domain distribution alignment can easily cause class misalignment (different classes are pulled together). Thus, we design a domain projection parameter θ_τ to directly transform the target domain data into a feature space close to the source domain data. Specifically, we first measure the similarity of samples between the target domain and the source domain, and then further pull the target domain samples and similar source domain samples closer.

Let A stand for the similarity matrix of samples in the query set from target domain to the support set from source domain. Then, D^A represents the diagonal matrix of all row-summing values of A . Formally, in each meta task, the optimization problem w.r.t. θ_τ can be written by:

$$\begin{aligned} &\min_{\theta_\tau} \sum_{i,k} A_{ik} \|Z_{T,i}^{\text{que}} \theta_\tau - Z_{S,k}^{\text{sup}}\|^2 + \gamma_p \|\theta_\tau\|^2 \\ &= \text{tr}(\theta_\tau^\top Z_\tau^{\text{sup} \top} D^A Z_\tau^{\text{sup}} \theta_\tau) - 2\text{tr}(\theta_\tau^\top Z_\tau^{\text{sup} \top} A Z_S^{\text{sup}}) + \gamma_p \|\theta_\tau\|^2, \end{aligned} \quad (9)$$

where $Z_{T,i}^{\text{que}} \theta_\tau$ represents the projected feature of the i -th target domain sample $Z_{T,i}^{\text{que}}$, and A_{ik} is its similarity to the k -th source domain sample $Z_{S,k}^{\text{sup}}$. We use the regularizer $\|\theta_\tau\|^2$ to prevent overfitting, and γ_p is a learnable regularization

Algorithm 1 Proposed E²MPL

Training Input: An auxiliary dataset including labeled \mathcal{S}_{aux} and unlabeled \mathcal{T}_{aux} , and learning rate β

Training Output: prompt parameters Θ

- 1: **while** not converged **do**
- 2: Sample a meta task consisting of D_i^{sup} and D_i^{que} from the auxiliary dataset.
- 3: *# obtain the feature embeddings*
 $Z_{S,i}^{\text{sup}} = f_e(X_{S,i}^{\text{sup}}; \Theta)$, $Z_{T,i}^{\text{que}} = f_e(X_{T,i}^{\text{que}}; \Theta)$
- 4: *# optimize classification parameter*
 $\theta_\omega^* \leftarrow$ closed-form solution of Eqn. (8).
- 5: *# optimize domain projection parameter*
 $\theta_\tau^* \leftarrow$ closed-form solution of Eqn. (11).
- 6: Predict the labels $\hat{Y}_{S,i}^{\text{que}}$ and $\hat{Y}_{T,i}^{\text{que}}$ of the query set by applying θ_ω^* and θ_τ^*
- 7: Solve Eqn. (6) by calculating its gradient w.r.t. Θ
- 8: *# update feature embedding parameter*
 $\Theta \leftarrow \Theta - \beta \nabla_\Theta (\mathcal{L}_c^{\text{meta}} + \lambda_d \mathcal{L}_d^{\text{meta}} + \lambda_f \mathcal{L}_f^{\text{meta}})$.
- 9: **end while**

Testing Input: D_S^{sup} and D_T^{que} in a new task and learned Θ

Testing Output: Prediction $\hat{Y}_{T,\text{new}}^{\text{que}}$ for this new task

- 1: Calculate $Z_{S,\text{new}}^{\text{sup}} = f_e(X_{S,\text{new}}^{\text{sup}}; \Theta)$ and
 $\theta_\omega^{\text{new}} \leftarrow Z_{S,\text{new}}^{\text{sup} \top} \left(Z_{S,\text{new}}^{\text{sup}} Z_{S,\text{new}}^{\text{sup} \top} + \gamma_\omega I \right)^{-1} Y_{S,\text{new}}^{\text{sup}}$.
- 2: Calculate $Z_{T,\text{new}}^{\text{que}} = f_e(X_{T,\text{new}}^{\text{que}}; \Theta)$ and
 $\theta_\tau^{\text{new}} \leftarrow Z_{T,\text{new}}^{\text{que} \top} \left(D^A Z_{T,\text{new}}^{\text{que}} Z_{T,\text{new}}^{\text{que} \top} + \gamma_p I \right)^{-1} A Z_{S,\text{new}}^{\text{sup}}$.
- 3: Predict the labels $\hat{Y}_{T,\text{new}}^{\text{que}}$ by using $Z_{T,\text{new}}^{\text{que}} \theta_\tau^{\text{new}} \theta_\omega^{\text{new}}$.

parameter. Then, by setting the partial derivation of Eq. (9) w.r.t. θ_τ as zero, we obtain

$$\begin{aligned} 2Z_\tau^{\text{que} \top} D^A Z_\tau^{\text{que}} \theta_\tau - 2Z_\tau^{\text{que} \top} A Z_S^{\text{sup}} + 2\gamma_p \theta_\tau &= 0, \\ (Z_\tau^{\text{que} \top} D^A Z_\tau^{\text{que}} + \gamma_p I_c) \theta_\tau &= Z_\tau^{\text{que} \top} A Z_S^{\text{sup}}. \end{aligned}$$

Thus, θ_τ has a closed-form solution, which can be written as

$$\theta_\tau^* = (Z_\tau^{\text{que} \top} D^A Z_\tau^{\text{que}} + \gamma_p I_c)^{-1} Z_\tau^{\text{que} \top} A Z_S^{\text{sup}}. \quad (10)$$

For computation efficiency, we leverage Woodbury identity to update the above solution as:

$$\theta_\tau^* = Z_\tau^{\text{que} \top} (D^A Z_\tau^{\text{que}} Z_\tau^{\text{que} \top} + \gamma_p I_n)^{-1} A Z_S^{\text{sup}}, \quad (11)$$

where the matrix A is calculated by $A_{ik} = e^{-\|Z_{T,i}^{\text{que}} - Z_{S,k}^{\text{sup}}\|^2}$. To avoid the value explosion caused by matrix multiplication, we alternately normalize the matrix A row by row and column by column until convergence. Note that alternating normalization of rows and columns not only improves the stability and efficiency of the calculation, but also reduces numerical instability when dealing with large-scale data.

In summary, the domain projection parameter θ_τ^* can be calculated in one step to narrow the domain gap. Thus, labeled data from the source domain can be leveraged to enhance the classification of unlabeled data in the target domain.

In this way, thank to closed-form solutions of θ_ω^* and θ_τ^* , the proposed E²MPL model can be efficiently trained among meta-tasks and quickly adapted to new tasks. The meta-train and meta-test process is summarized in Algorithm 1. During

the meta-train, given pretrained encoder and the sampled meta-task i from an auxiliary dataset, the algorithm first calculates the optimal parameters θ_ω^* and $\theta_{\mathcal{T}}^*$ for classification and domain alignment via the closed-form solutions and then validates them in the query set. Afterwards, the resulted meta prompt loss is used to update the prompt parameters Θ by gradient descent. During the meta-test on a new task, with the learned prompts, the algorithm calculates the new $\theta_\omega^{\text{new}}$ and $\theta_{\mathcal{T}}^{\text{new}}$ to test the classification in the target domain.

IV. EXPERIMENTS

In this section, we demonstrate the effectiveness of our proposed E²MPL. We first introduce datasets, implementation details and meta-task setting. Next, we compare the proposed method with other related methods to evaluate the ability of adaptation to target domain, and task generalization to unseen categories. Then, we provide the ablation studies to explore the contribution of each component in E²MPL. We also design a comparison of training time and provide analysis to show the efficacy of the proposed method.

A. Datasets and Implementation

We experiment on the benchmark dataset *DomainNet* [55], which has usually been used for FS-UDA methods. It was released in 2019 for the research of multi-source domain adaptation [55], and consists of six distinct domains: *quickdraw*, *clipart*, *real*, *sketch*, *painting*, *infograph*, each containing a diverse array of images categorized into 345 object classes. In our experiments, we use the first five domains and first select any two of the five domains as the source and target domains, respectively, thus forming 20 different source-to-target domain adaptation tasks. Then, we discard the 40 categories that contain less than 20 images for the two domains. Finally, we randomly split the images of the remaining 308 categories into images of 217 categories, 43 categories, and 48 categories, and adjusted the size of these images to 224×224 pixels for meta-training (forming the auxiliary dataset), model validation and testing new tasks, respectively.

Implementation details. Our experiments are carried out with a single NVIDIA GTX 3090 GPU and PyTorch. The network architecture of our E²MPL consists of two components: the backbone and the prompt module. We utilize two different backbones: a pretrained ViT-B/32 (CLIP) with prompts used in [56] and a pretrained 12-layer ResNet network (ResNet-12) used in [57]. For pretraining of the CLIP, we only used the fixed visual encoder ViT-B/32, and to speed up training, we used the head layer to reduce the data feature dimension from 512 to 128. For pretraining of the ResNet-12, we use ResNet-12 as a feature extractor and full connected layer as a classifier for pretraining on *miniImageNet*. In addition, since the feature extraction capability of ResNet-12 is not as powerful as that of CLIP, we introduce a data augmentation method [58] [59] [60] when the backbone is ResNet-12. The prompt module consists mainly of domain-shared prompts, task-specific prompts, and a head layer. Through experiments, we found that the best experimental results were achieved when the domain-shared prompt was composed of four prompts. Therefore, the size of

the domain-shared prompt is 4×768 (768 is the dimension of the image patch). For task-specific prompts, we also use ResNet-12 to pre-train on *miniImageNet* to obtain prior knowledge. Afterwards, we train E²MPL for 10 epochs and perform episodic training on 1000 episodes for each epoch. In each episode, a meta-task is randomly constructed from the dataset to train our meta-prompt model. For model training, we use the Adam solver with the related gradient weights of 0.5 and 0.999, and the learning rate is empirically set as 0.005. Both λ_d and λ_f in Eqn. (6) are set to 0.01 for *DomainNet*. The γ_ω and γ_p in Eqns. (8) and (11) are automatically updated along with the meta prompt learner through the outer optimization. During the meta-test, we randomly select 3600 tasks to calculate the averaged top-1 accuracy as the evaluation criterion.

To realize the 5-way K -shot UDA setting, in each meta task, we first randomly samples $5 * (K + 15)$ labeled samples from the source domain and 75 unlabeled samples from the target domain, which are derived from five categories randomly selected equally. Then, the $(K + 15)$ source domain samples in each category are randomly partitioned into K for the support set and 15 for the query set, while the 75 target domain samples are used for the query set. For each meta-test task, its support and query sets have the same set of five new categories. The support set contains 5K labeled source domain samples for classifier update, while the query set contains 75 unlabeled target domain samples for performance evaluation.

B. Comparison Methods and Results

We compare our E²MPL with twenty-three related methods on *DomainNet* in Table I. This includes three popular UDA methods (*i.e.*, MCD [12], ADDA [19] and DWT [16]), three meta-learning methods (*i.e.*, MAML [43], R2D2 [52] and Meta-ticket [61]), seven FSL methods (*i.e.*, baseline/baseline++ [62], ProtoNet [47], DN4 [48], ADM [63], FEAT [49] and DeepEMD [64]), as well as two FS-UDA methods (*i.e.*, IMSE [1] and TSECS [3]). Then, we evaluate variants of meta-learning methods by integrating ADDA for domain adaptation [19], *i.e.*, ADDA+MAML, ADDA+R2D2 and ADDA+Meta-ticket. In addition, we also combine the aforementioned five FSL methods with ADDA [19], which are abbreviated as ADDA+ProtoNet, ADDA+DN4, ADDA+ADM, ADDA+FEAT, and ADDA+DeepEMD, respectively. For most of the methods involved in this comparison, we utilize their publicly available open-source codes and configure their optimal parameters for implementation. Furthermore, for fair comparison, all comparison experiments are conducted on the same data, and we modify these compared methods for the FS-UDA setting as follows.

For the UDA methods of MCD, ADDA and DWT, we first train a UDA model on the whole auxiliary dataset. Once the model is trained, we proceed to adapt the model to new FS-UDA tasks by fine-tuning the fully connected layers, ensuring that it performs well on the new task during testing. **For the meta-learning methods of MAML, R2D2 and Meta-ticket**, we directly train a model over meta-tasks by only leveraging their source domain data for few-shot classification to optimize the model parameters, and then migrate the models

TABLE I: Comparison of our E²MPL and the baseline methods for the FS-UDA setting. The classification accuracy (%) of target domain samples are averaged over 3600 new tasks under the 5-way, K -shot setting. The best performances are shown in bold.

5-way, 1-shot, backbone: CLIP (ViT-B/32)											
Methods	skt \leftrightarrow rel \rightarrow / \leftarrow	skt \leftrightarrow qdr \rightarrow / \leftarrow	skt \leftrightarrow pnt \rightarrow / \leftarrow	skt \leftrightarrow cli \rightarrow / \leftarrow	rel \leftrightarrow qdr \rightarrow / \leftarrow	rel \leftrightarrow pnt \rightarrow / \leftarrow	rel \leftrightarrow cli \rightarrow / \leftarrow	qdr \leftrightarrow pnt \rightarrow / \leftarrow	qdr \leftrightarrow cli \rightarrow / \leftarrow	pnt \leftrightarrow cli \rightarrow / \leftarrow	avg -
MCD [12]	71.64/63.03	39.71/38.02	63.24/60.26	59.52/65.28	34.97/59.86	67.19/68.65	65.45/77.64	43.05/31.39	57.24/37.41	59.94/69.61	56.66
ADDA [19]	73.97/64.36	42.17/39.73	61.85/61.26	60.03/67.56	35.44/63.72	69.09/69.93	65.14/76.51	43.61/34.68	58.40/38.13	66.92/72.18	58.23
DWT [16]	73.21/63.86	43.59/42.45	63.94/65.57	61.06/68.36	35.49/62.81	69.68/71.32	67.83/79.15	48.02/35.19	58.87/39.47	61.38/74.79	59.30
MAML [43]	77.88/76.93	51.34/50.25	69.67/67.48	75.89/76.29	48.39/51.69	75.86/74.82	79.74/80.25	44.04/43.48	53.31/51.98	68.86/68.95	64.36
R2D2 [52]	72.10/79.19	56.89/58.10	71.09/72.69	80.32/79.95	51.84/55.06	76.58/79.17	82.67/84.29	48.57/45.70	60.63/55.79	74.79/74.12	67.98
Meta-ticket [61]	79.19/78.98	56.23/53.94	71.68/69.37	78.26/78.67	51.48/52.89	75.91/75.05	80.72/81.22	45.63/43.51	56.97/57.49	70.75/68.42	66.32
baseline [62]	65.16/59.05	40.59/39.30	56.15/55.40	62.90/65.22	37.55/39.47	55.44/62.23	63.70/72.52	33.35/34.38	40.90/40.44	57.08/59.52	52.02
baseline++ [62]	73.00/74.00	45.49/53.68	65.32/64.32	70.64/71.44	43.98/50.86	72.30/69.29	76.70/77.81	42.33/36.79	53.86/46.01	65.18/65.50	60.93
ProtoNet [47]	77.40/75.97	51.60/50.87	69.42/70.04	76.83/77.23	45.29/49.60	73.06/75.18	78.85/80.93	40.51/44.61	52.88/51.51	71.53/69.99	64.17
DN4 [48]	72.97/65.17	39.39/57.99	63.68/61.31	62.45/69.55	34.25/61.19	68.70/70.04	66.79/78.79	52.11/34.58	59.93/40.35	60.94/77.00	59.86
ADM [63]	73.25/65.94	42.81/59.42	64.93/64.57	64.39/72.67	45.82/60.96	70.86/72.63	67.04/79.91	48.77/35.14	59.21/43.87	62.90/76.56	61.58
FEAT [49]	74.75/67.74	44.59/58.60	66.19/62.80	69.90/72.51	51.18/60.71	69.69/71.06	77.12/79.59	47.37/43.73	60.67/52.41	64.39/70.01	63.25
DeepEMD [64]	73.54/67.02	43.15/58.48	65.73/63.62	68.09/73.55	40.37/61.43	69.30/71.97	68.46/78.74	53.50/38.25	61.38/42.84	63.76/73.53	61.84
ADDA+MAML	81.33/79.95	57.63/52.01	70.10/70.73	77.16/73.14	56.81/55.01	76.40/78.32	80.69/81.04	49.34/48.52	57.84/56.99	73.92/72.33	67.46
ADDA+R2D2	79.01/79.15	57.84/58.43	71.44/71.82	78.56/78.43	58.91/58.74	77.47/78.13	82.43/83.02	49.51/52.41	60.70/59.49	74.12/73.96	69.18
ADDA+Meta-ticket	81.49/80.30	62.03/56.74	76.45/70.14	79.82/78.41	58.77/52.94	76.18/75.16	81.08/81.51	59.39/53.22	56.67/56.25	71.43/69.85	68.84
ADDA+ProtoNet	82.96/81.45	56.18/54.29	70.52/71.14	79.32/77.35	52.51/55.76	75.09/79.47	79.38/82.65	44.36/45.17	53.81/53.05	71.94/70.95	66.87
ADDA+DN4	79.63/71.77	44.19/59.26	67.94/65.76	64.47/75.64	39.34/65.72	72.98/74.77	69.26/80.35	59.21/37.92	61.29/47.12	65.78/79.29	64.09
ADDA+ADM	80.56/72.12	46.80/61.48	69.84/65.39	68.06/77.28	49.13/62.59	74.16/76.42	72.12/81.44	57.95/38.64	60.85/49.17	67.81/79.35	65.56
ADDA+FEAT	81.39/74.36	46.51/60.13	68.70/67.65	71.94/75.40	55.19/63.97	73.27/76.13	78.04/80.97	58.74/45.38	60.48/54.13	69.46/75.62	66.90
ADDA+DeepEMD	80.31/72.65	47.81/62.25	67.82/66.74	70.45/74.83	47.61/65.39	74.59/76.27	74.32/81.95	61.20/46.73	62.55/50.31	67.84/78.54	66.51
IMSE [1]	73.12/64.71	39.30/57.28	63.75/61.39	64.28/69.30	33.94/61.03	68.37/70.07	66.27/79.01	52.11/34.12	59.28/40.02	60.87/68.47	59.34
TSECS [3]	77.34/79.59	68.87/65.30	70.65/70.26	78.51/79.97	56.09/64.58	76.51/89.51	81.64/83.79	53.21/56.69	67.92/75.17	69.98/73.58	71.96
E ² MPL	94.80/92.83	78.92/80.12	87.08/90.55	94.46/92.79	82.37/86.72	92.42/94.50	96.97/97.03	73.15/72.14	86.43/80.54	92.55/89.76	87.81
5-way, 5-shot, backbone: CLIP (ViT-B/32)											
MCD [12]	86.50/73.38	57.82/64.20	73.27/74.42	75.62/75.11	48.89/62.46	70.66/76.07	78.83/86.34	62.53/38.58	62.19/46.49	73.24/80.69	68.37
ADDA [19]	86.62/75.89	61.81/66.13	76.25/75.33	78.99/78.12	54.63/75.82	75.38/81.71	77.57/88.72	68.37/42.51	73.65/46.59	76.92/80.79	72.09
DWT [16]	86.91/73.56	63.26/70.31	76.85/74.57	80.78/81.91	56.80/78.52	76.57/82.22	81.06/89.15	65.96/43.91	76.74/49.69	77.08/82.21	73.41
MAML [43]	92.19/85.51	56.49/58.15	80.70/81.07	88.29/86.46	52.39/54.10	84.69/88.42	89.98/92.44	45.72/50.76	59.51/56.84	84.19/80.15	73.40
R2D2 [52]	91.52/86.54	62.30/67.19	82.24/84.64	90.55/86.54	56.56/62.13	84.70/90.80	91.06/93.67	53.40/53.83	70.48/64.36	86.86/82.84	77.11
Meta-ticket [61]	90.18/81.69	61.07/65.42	81.70/81.99	89.26/86.39	57.96/56.35	85.59/89.64	89.53/93.26	51.34/54.89	60.43/61.82	84.24/80.40	75.16
baseline [62]	82.17/72.82	49.41/47.02	71.33/70.81	80.69/80.38	42.96/47.36	68.50/78.68	78.33/87.71	38.70/40.78	48.93/48.09	72.61/72.37	63.98
baseline++ [62]	90.48/85.36	57.92/66.61	80.68/80.93	88.32/85.94	50.93/65.46	83.70/86.12	89.52/92.02	53.52/45.19	67.74/55.97	81.96/78.70	74.35
ProtoNet [47]	89.06/83.98	57.87/61.08	79.25/82.25	89.28/86.06	51.44/55.45	80.80/89.68	88.15/90.60	46.52/50.58	63.72/58.36	83.76/78.61	73.33
DN4 [48]	89.89/78.62	63.10/74.23	79.56/77.88	81.57/84.79	40.10/79.77	80.84/85.79	80.76/92.85	67.99/42.82	77.52/49.15	78.28/82.13	74.38
ADM [63]	87.40/76.43	64.57/75.89	73.05/79.92	81.98/85.35	42.02/76.12	81.90/79.72	72.26/89.67	62.91/43.17	76.84/58.43	81.72/83.20	73.63
FEAT [49]	89.92/79.64	67.38/77.60	81.59/80.23	82.37/85.76	46.10/82.39	84.97/87.22	84.65/93.33	68.72/48.48	79.58/57.78	83.94/85.81	77.37
DeepEMD [64]	91.23/82.89	68.31/77.12	82.06/81.11	84.75/84.39	45.91/83.85	84.74/89.58	85.72/92.86	67.21/49.27	81.53/56.49	83.61/84.95	77.88
ADDA+MAML	93.13/88.58	66.80/62.32	82.27/83.69	89.24/87.00	57.57/60.76	85.01/90.39	90.89/92.29	46.26/53.32	67.98/62.25	85.65/83.34	76.44
ADDA+R2D2	90.60/86.08	68.29/66.84	83.20/84.22	89.77/87.01	67.08/67.93	85.72/90.60	90.46/91.97	58.61/62.64	71.48/68.53	87.25/83.06	79.07
ADDA+Meta-ticket	92.21/82.47	66.85/69.76	80.64/82.03	89.34/86.29	63.97/67.46	86.52/89.39	90.04/93.98	62.65/61.78	71.88/71.95	85.62/80.74	78.78
ADDA+ProtoNet	93.29/85.61	64.27/66.85	80.34/83.62	91.57/86.73	52.35/55.64	82.68/92.87	89.36/91.17	47.29/50.32	65.42/59.12	83.91/79.46	75.09
ADDA+DN4	92.75/84.69	65.23/71.94	84.31/83.04	82.70/88.57	45.62/79.95	82.92/90.01	84.27/93.49	68.48/46.91	80.15/56.11	81.93/85.41	77.42
ADDA+ADM	92.93/83.14	66.75/74.45	81.66/84.72	83.19/88.87	45.95/77.37	83.57/90.98	85.75/93.57	65.42/49.87	78.57/60.21	82.32/85.53	77.74
ADDA+FEAT	94.07/81.99	71.72/77.53	86.74/85.92	83.68/87.24	47.29/84.61	85.18/91.24	87.89/94.01	69.15/50.39	81.33/61.78	85.19/86.82	79.69
ADDA+DeepEMD	93.24/85.96	70.39/78.29	83.17/83.95	87.36/85.74	47.87/84.69	86.51/91.55	86.87/93.17	67.44/53.52	81.97/59.24	85.42/84.79	79.56
IMSE [1]	89.70/78.39	49.58/74.00	79.55/77.78	82.37/84.46	40.45/79.86	81.06/85.98	81.04/93.23	67.71/43.41	76.82/49.56	77.25/81.96	73.71
TSECS [3]	94.78/90.30	68.38/77.26	85.55/87.50	93.78/90.31	65.91/81.73	86.43/95.04	93.46/95.94	68.33/58.56	85.66/70.81	89.25/84.77	83.19
E ² MPL	98.19/94.76	85.02/89.20	93.19/93.87	97.01/95.33	85.95/93.25	93.15/98.12	97.25/98.01	80.69/82.84	91.95/87.42	96.56/93.10	92.24

to the target domain to evaluate the adaptability of model on the new task in the meta-testing phase. **For the few-shot learning methods of baseline, baseline++, ProtoNet, DN4, ADM, FEAT and DeepEMD** applied for our setting, we train a pre-trained model on the source domain data, and then the pre-trained model is adapted to the target domain data. **For the eight combination methods**, taking ADDA+MAML as an example, we pre-train the MAML on the source domain to learn effective feature representations. Simultaneously, we employ an unsupervised domain adaptation strategy like Adversarial Discriminative Domain Adaptation (ADDA) to align the source and target domains. Next, **for the FS-UDA methods of IMSE and TSECS**, we can directly evaluate them since their experimental setting is the same as ours.

To better demonstrate the advantages of the E²MPL, we first use the pre-trained model CLIP as the backbone, and then report the average classification accuracy of target domain samples over 3600 tasks tested. As seen in Table I, our E²MPL consistently and significantly achieves the best performance with only a few parameters learned, compared to the other methods on *DomainNet* for both 1-shot and 5-shot tasks. It shows the effectiveness of our E²MPL method for FS-UDA. To verify that our method is not only applicable to large pre-trained models (CLIP), but also works well on other traditional models, *i.e.*, ResNet-12. As shown in Table II, using ResNet-12 as the backbone, we compare E²MPL with twenty-one related methods on *DomainNet*: three UDA methods (*i.e.*, MCD, ADDA and DWT), three meta-learning

TABLE II: Comparison of our E²MPL and the baseline methods for the FS-UDA setting. The classification accuracy (%) of target domain samples are averaged over 3600 new tasks under the 5-way, K -shot setting. The best performances are shown in bold.

5-way, 1-shot, backbone: ResNet-12											
Methods	skt \leftrightarrow rel \rightarrow / \leftarrow	skt \leftrightarrow qdr \rightarrow / \leftarrow	skt \leftrightarrow pnt \rightarrow / \leftarrow	skt \leftrightarrow cli \rightarrow / \leftarrow	rel \leftrightarrow qdr \rightarrow / \leftarrow	rel \leftrightarrow pnt \rightarrow / \leftarrow	rel \leftrightarrow cli \rightarrow / \leftarrow	qdr \leftrightarrow pnt \rightarrow / \leftarrow	qdr \leftrightarrow cli \rightarrow / \leftarrow	pnt \leftrightarrow cli \rightarrow / \leftarrow	avg -
MCD [12]	48.07/37.74	38.90/34.51	39.31/35.59	51.43/38.98	24.17/29.85	43.36/47.32	44.71/45.68	26.14/25.02	42.00/34.69	39.49/37.28	38.21
ADDA [19]	48.82/46.06	38.42/40.43	42.52/39.88	50.67/47.16	31.78/35.47	43.93/45.51	46.30/47.66	26.57/27.46	46.51/32.19	39.76/41.24	40.91
DWT [16]	49.43/38.67	40.94/38.00	44.73/39.24	52.02/50.69	29.82/29.99	45.81/50.10	52.43/51.55	24.33/25.90	41.47/39.56	42.55/40.52	41.38
MAML [43]	43.84/31.19	25.67/23.12	32.88/28.69	33.32/31.69	23.84/23.08	39.21/36.14	35.58/36.35	22.57/22.95	25.63/23.51	29.79/28.97	29.90
R2D2 [52]	38.48/33.63	26.16/27.67	33.47/31.17	35.92/33.82	23.80/24.66	39.65/40.46	38.49/40.92	23.39/23.05	27.36/25.34	31.01/31.40	31.49
Meta-ticket [61]	44.12/35.39	28.79/29.48	33.39/31.08	34.85/34.61	26.28/26.85	43.64/45.54	39.85/40.72	23.31/23.98	28.27/25.02	31.48/32.68	32.97
ProtoNet [47]	50.48/43.15	41.20/32.63	46.33/39.69	53.45/48.17	32.48/25.06	49.06/50.30	49.98/51.95	22.55/28.76	36.93/40.98	40.13/41.10	41.21
DN4 [48]	52.42/47.29	41.46/35.24	46.64/46.55	54.10/51.25	33.41/27.48	52.90/53.24	53.84/52.84	22.82/29.11	36.88/43.61	47.42/43.81	43.61
ADM [63]	49.36/42.27	40.45/30.14	42.62/36.93	51.34/46.64	32.77/24.30	45.13/51.37	46.80/50.15	21.43/30.12	35.64/43.33	41.49/40.02	40.11
FEAT [49]	51.72/45.66	40.29/35.45	47.09/42.99	53.69/50.59	33.81/27.58	52.74/53.82	53.21/53.31	23.10/29.39	37.27/42.54	44.15/44.49	43.14
DeepEMD [64]	52.24/46.84	42.12/34.77	46.64/43.89	55.10/49.56	34.28/28.02	52.73/53.26	54.25/54.91	22.86/28.79	37.65/42.92	44.11/44.38	43.46
ADDA+MAML	41.01/31.23	24.60/23.56	30.14/28.16	33.40/30.43	22.93/25.64	38.77/36.10	37.19/38.72	23.98/25.46	26.72/28.97	31.16/31.96	30.50
ADDA+R2D2	36.51/33.57	23.73/23.35	31.16/29.55	33.55/32.83	23.67/22.42	39.80/37.69	39.31/38.90	22.11/21.90	23.57/23.14	30.23/31.98	29.95
ADDA+Meta-ticket	43.28/36.38	25.71/24.64	33.41/31.27	38.81/33.97	25.62/26.74	45.33/44.21	40.54/41.68	24.79/25.16	28.29/25.62	31.93/32.85	33.01
ADDA+ProtoNet	51.30/43.43	41.79/35.40	46.02/41.40	52.68/48.91	37.28/27.68	50.04/49.68	49.83/52.58	23.72/32.03	38.54/44.14	41.06/41.59	42.45
ADDA+DN4	53.04/46.08	42.64/36.46	46.38/47.08	54.97/51.28	34.80/29.84	53.09/54.05	54.81/55.08	23.67/31.62	42.24/45.24	46.25/44.40	44.65
ADDA+ADM	51.87/45.08	43.91/32.38	47.48/43.37	54.81/51.14	35.86/28.15	48.88/51.61	49.95/54.29	23.95/33.30	43.59/48.21	43.52/43.83	43.76
ADDA+FEAT	52.72/46.08	47.00/36.94	47.77/45.01	56.77/52.10	36.32/30.50	49.14/52.36	52.91/53.86	24.76/35.38	44.66/48.82	45.03/45.92	45.20
ADDA+DeepEMD	53.98/47.55	44.64/36.19	46.29/45.14	55.93/50.45	37.47/30.14	52.21/53.32	54.86/54.80	23.46/32.89	39.06/46.76	45.39/44.65	44.75
IMSE [1]	57.21/51.30	49.71/40.91	50.36/46.35	59.44/54.06	44.43/36.55	52.98/55.06	57.09/57.98	30.73/38.70	48.94/51.47	47.42/46.52	48.86
TSECS [3]	65.00/58.22	62.25/51.97	56.51/53.70	69.45/64.59	56.66/49.82	58.76/63.18	67.98/67.89	38.26/46.15	60.51/69.03	54.40/52.76	58.20
E ² MPL	67.13/66.56	62.51/52.82	59.61/61.09	72.35/67.17	57.41/46.32	65.92/68.60	69.39/73.83	36.19/49.15	59.04/66.29	62.67/61.17	61.26
5-way, 5-shot, backbone: ResNet-12											
MCD [12]	66.42/47.73	51.84/39.73	54.63/47.75	72.17/53.23	28.02/33.98	55.74/66.43	56.80/63.07	28.71/29.17	50.46/45.02	53.99/48.24	49.65
ADDA [19]	66.46/56.66	51.37/42.33	56.61/53.95	69.57/65.81	35.94/36.87	58.11/63.56	59.16/65.77	23.16/33.50	41.94/43.40	55.21/55.86	51.76
DWT [16]	67.75/54.85	48.59/40.98	55.40/50.64	69.87/59.33	36.19/36.45	60.26/68.72	62.92/67.28	22.64/32.34	47.88/50.47	49.76/52.52	51.74
MAML [43]	52.59/38.76	28.04/28.42	38.46/34.98	43.28/40.45	27.52/27.36	50.49/52.71	44.63/53.86	23.81/24.25	28.92/29.31	38.11/37.73	37.18
R2D2 [52]	50.51/39.78	29.31/28.78	39.48/36.88	44.07/40.44	29.43/27.81	50.51/53.37	46.62/54.62	24.79/26.53	31.63/32.15	39.07/39.54	38.27
Meta-ticket [61]	54.62/41.38	30.72/31.47	43.82/38.69	46.12/41.52	30.32/29.17	51.60/54.54	47.28/56.36	25.78/26.93	32.78/34.17	40.12/41.77	39.99
ProtoNet [47]	65.07/56.21	52.65/39.75	55.13/52.77	65.43/62.62	37.77/31.01	61.73/66.85	63.52/66.45	20.74/30.55	45.49/55.86	53.60/52.92	51.80
DN4 [48]	63.89/51.96	48.23/38.68	52.57/51.62	62.88/58.33	37.25/29.56	58.03/64.72	61.10/62.25	23.86/33.03	41.77/49.46	50.63/48.56	49.41
ADM [63]	66.25/54.20	53.15/35.69	57.39/55.60	71.73/63.42	44.61/24.83	59.48/69.17	62.54/67.39	21.13/38.83	42.74/58.36	56.34/52.83	52.78
FEAT [49]	67.91/58.56	52.27/40.97	59.01/55.44	69.37/65.95	40.71/28.65	63.85/71.25	65.76/68.96	23.73/34.02	42.84/53.56	57.95/54.84	53.78
DeepEMD [64]	67.96/58.11	53.34/39.70	59.31/56.60	70.56/64.60	39.70/29.95	62.99/70.93	65.07/69.06	23.86/34.34	45.48/53.93	57.60/55.61	53.93
ADDA+MAML	52.56/39.25	29.99/27.63	40.89/37.91	45.40/45.21	27.58/27.84	50.63/53.30	48.77/50.46	23.11/22.18	27.12/26.69	37.55/40.83	37.75
ADDA+R2D2	52.15/41.34	30.13/26.48	44.76/38.33	46.97/45.44	26.79/27.74	49.87/50.82	49.98/51.69	23.76/23.52	30.75/30.07	39.72/42.03	38.12
ADDA+Meta-ticket	56.31/42.70	31.52/32.22	43.64/40.14	48.97/47.95	28.64/29.37	54.39/57.69	53.73/56.91	25.85/26.62	32.78/34.10	40.12/41.17	40.94
ADDA+ProtoNet	66.11/58.72	52.92/43.60	57.23/53.90	68.44/61.84	45.59/38.77	60.94/69.47	66.30/66.10	25.45/41.30	46.67/56.22	58.20/52.65	54.52
ADDA+DN4	63.40/52.40	48.37/40.12	53.51/49.69	64.93/58.39	36.92/31.03	57.08/65.92	60.74/63.13	25.36/34.23	48.52/51.19	52.16/49.62	50.33
ADDA+ADM	64.64/54.65	52.56/33.42	56.33/54.85	70.70/63.57	39.93/27.17	58.63/68.70	61.96/67.29	21.91/39.12	41.96/59.03	55.57/53.39	52.27
ADDA+FEAT	67.80/56.71	60.33/43.34	57.32/58.08	70.06/64.57	44.13/35.62	62.09/70.32	57.46/67.77	29.08/44.15	49.64/63.38	57.95/54.84	55.56
ADDA+DeepEMD	68.52/59.28	56.78/40.03	58.18/57.86	70.83/65.39	42.63/32.18	63.82/71.54	66.51/69.21	26.89/42.33	47.00/57.92	57.81/55.23	55.49
IMSE [1]	70.46/61.09	61.57/46.86	62.30/59.15	76.13/67.27	53.07/40.17	64.41/70.63	67.60/71.76	33.44/48.89	53.38/65.90	61.28/56.74	59.60
TSECS [3]	78.23/70.44	77.90/55.77	66.70/68.03	83.82/74.28	64.33/55.16	68.40/79.74	78.23/77.69	39.74/63.02	67.99/80.31	73.67/61.63	69.25
E ² MPL	80.28/69.77	77.61/60.64	71.27/72.34	86.00/76.34	69.10/53.86	72.37/84.71	83.15/85.03	44.89/64.32	62.77/78.54	77.52/71.38	71.90

methods (*i.e.*, MAML, R2D2, Meta-ticket), and five popular few-shot methods (*i.e.*, ProtoNet, DN4, ADM, FEAT and DeepEMD). We also combine the few-shot methods with ADDA, *e.g.*, ADDA+MAML, ADDA+R2D2. Meanwhile, we also compare and analyze E²MPL with IMSE and TSECS designed specifically for FS-UDA.

In general, whether based on CLIP or ResNet-12, E²MPL has a great improvement over other methods. This is due to the fact that our meta-prompt learning framework can learn meta-prompts shared between tasks as well as task-specific prompts to quickly adapt to new tasks, thus improving the model generalizability.

Comparison analysis between our E²MPL and other methods. Through the observation and analysis, it is found that the reason why the UDA, meta learning and FSL methods are not effective is that the UDA models are likely to overfit the limited labeled samples, and the meta learning

and FSL methods fail to deal with the issue of domain gaps. Even traditional meta-learning method combined with UDA methods (ADDA+MAML) may not be able to effectively deal with the FS-UDA problem, because the features and distributions of the source data can interfere with learning in the target domain, making it difficult for the model to extract effective, representative features. As a result, the model may become confined to the limitations of the training data, leading to overfitting. Therefore, simply combining these two approaches is insufficient to tackle the complex challenges, necessitating more refined strategies to address the dual issues of task generalization and domain gaps. E²MPL fixed the pre-trained model, preserving the model's ability to learn general features. Additionally, through meta-prompt learning strategies, the model gained the capability to learn domain-shared features as well as task-specific discriminative features, significantly reducing the risk of model overfitting.

TABLE III: Comparison of related prompt learning methods. ‘*’ indicates that its prompt module replaces our prompts in our E²MPL meta-prompt learning framework as it cannot be used directly.

5-way, 1-shot, backbone: CLIP(ViT-B/32)											
Methods	skt \leftrightarrow rel \rightarrow / \leftarrow	skt \leftrightarrow qdr \rightarrow / \leftarrow	skt \leftrightarrow pnt \rightarrow / \leftarrow	skt \leftrightarrow cli \rightarrow / \leftarrow	rel \leftrightarrow qdr \rightarrow / \leftarrow	rel \leftrightarrow pnt \rightarrow / \leftarrow	rel \leftrightarrow cli \rightarrow / \leftarrow	qdr \leftrightarrow pnt \rightarrow / \leftarrow	qdr \leftrightarrow cli \rightarrow / \leftarrow	pnt \leftrightarrow cli \rightarrow / \leftarrow	avg -
DAM-VP	81.79/78.99	56.74/57.25	73.19/74.64	81.52/81.59	52.73/55.68	77.64/81.28	83.69/85.92	47.30/47.18	59.24/55.96	76.44/75.66	69.22
ProMetaR*	93.45/89.81	68.52/76.40	83.81/86.01	87.89/90.06	69.75/81.77	89.00/92.78	93.63/94.66	66.79/65.42	81.53/74.49	88.67/86.24	83.03
PGN*	92.52/90.38	73.47/77.35	84.95/86.57	91.44/90.08	73.44/81.59	88.59/92.22	94.06/95.03	69.03/66.01	83.58/77.46	89.10/87.30	84.21
VPT*	93.77/91.24	74.53/78.56	86.90/87.84	93.13/91.03	77.78/82.43	89.50/92.89	94.11/95.55	70.43/69.52	83.82/78.75	89.86/88.35	85.50
E ² MPL	94.80/92.83	78.92/80.12	87.08/90.55	94.46/92.79	82.37/86.72	92.42/94.50	96.97/97.03	73.15/72.14	86.43/80.54	92.55/89.76	87.81

5-way, 5-shot, backbone: CLIP (ViT-B/32)											
Methods	skt \leftrightarrow rel \rightarrow / \leftarrow	skt \leftrightarrow qdr \rightarrow / \leftarrow	skt \leftrightarrow pnt \rightarrow / \leftarrow	skt \leftrightarrow cli \rightarrow / \leftarrow	rel \leftrightarrow qdr \rightarrow / \leftarrow	rel \leftrightarrow pnt \rightarrow / \leftarrow	rel \leftrightarrow cli \rightarrow / \leftarrow	qdr \leftrightarrow pnt \rightarrow / \leftarrow	qdr \leftrightarrow cli \rightarrow / \leftarrow	pnt \leftrightarrow cli \rightarrow / \leftarrow	avg -
DAM-VP	90.33/84.22	60.12/62.56	81.78/83.46	89.66/83.72	59.87/64.61	81.55/90.81	87.12/91.05	65.76/62.64	68.92/58.70	86.61/79.73	76.66
ProMetaR*	95.39/91.50	79.47/79.75	88.30/89.67	94.10/91.74	77.32/85.73	90.22/95.27	95.03/96.28	72.70/72.33	87.75/80.13	92.45/88.11	87.16
PGN*	96.37/92.26	81.63/81.78	90.00/91.26	94.81/92.57	80.07/85.51	91.01/96.09	95.50/96.92	73.85/76.09	85.66/81.72	94.35/90.55	88.40
VPT*	96.74/93.13	82.74/82.64	90.58/92.24	95.27/93.57	81.28/89.29	91.97/96.59	96.15/97.07	74.95/77.81	88.33/83.22	94.82/90.94	89.46
E ² MPL	98.19/94.76	85.02/89.20	93.19/93.87	97.01/95.33	85.95/93.25	93.15/98.12	97.25/98.01	80.69/82.84	91.95/87.42	96.56/93.10	92.24

TABLE IV: Ablation study of the domain-shared and task-specific prompts designed in our E²MPL (backbone CLIP), where **all** (-skt) \Rightarrow **skt** indicates the average accuracy when other domains except for *sketch* are the source domain and *sketch* is the target domain.

domain-shared	task-specific	all(-skt) \Rightarrow skt		all(-rel) \Rightarrow rel		all(-qdr) \Rightarrow qdr		all(-pnt) \Rightarrow pnt		all(-cli) \Rightarrow cli	
		1-shot	5-shot	1-shot	5-shot	1-shot	5-shot	1-shot	5-shot	1-shot	5-shot
✓	✓	83.93	88.10	87.92	92.77	71.13	77.43	79.17	84.91	87.22	92.25
		88.05	91.89	92.04	95.81	76.57	83.73	84.38	89.08	91.03	94.67
		87.26	87.34	93.79	94.97	76.72	81.89	82.65	87.86	89.64	92.91
✓	✓	89.07	93.29	93.26	96.89	78.49	85.31	85.60	90.03	92.60	95.69

Comparison analysis between the two backbones CLIP and ResNet. Also, it is obvious that using CLIP as a backbone can better leverage the advantages of E²MPL, resulting in more significant improvements compared to ResNet. This may be due to CLIP pre-trained on large-scale datasets, which provides it with richer semantic knowledge. By optimizing the prompts alone, the model retains the ability to learn general features while also acquiring the key characteristics of new tasks. Nevertheless, using ResNet as a backbone, E²MPL still performs better on the FS-UDA problem than methods like IMSE and TSECS. This is because the meta-prompt framework provides prompt enhancements for new tasks, where prompts learned from previous tasks can assist in the learning of new tasks, thereby guiding the approach.

C. Evaluation of Prompt Learning

Comparison of prompt learning methods. To fully demonstrate the advantage of the designed prompts in our current work, we investigated our method with some previous prompt learning methods, including VPT [4], PGN [33], DAM-VP [6] and ProMetaR [8]. Given that these methods cannot be used directly in our setting, we have to put their prompt approach in our E²MPL meta-prompt learning framework, substituting for our domain-shared prompts and task-specific prompts. The classification accuracies obtained in 5-way 1-shot and 5-way 5-shot setting are shown in **Table III**. As can be seen, our method achieves the best performance, which indicates the efficacy of our designed domain-shared prompts and task-specific prompts.

Ablation study of the prompt components. To better demonstrate the contributions of each component of our prompts, we evaluated the performance of each prompt component in Table IV, where **all** (-skt) \Rightarrow **skt** indicates the average

accuracy when other domains except for *sketch* are the source domain and *sketch* is the target domain. The first line of Table IV is the baseline, which is to freeze the CLIP and not to use any prompts. The second line uses only domain-shared prompts, which helps the model learn a more generalized representation of features, thereby mitigating domain gaps. The third line is the use of task-specific prompts, which are obtained by passing image data through a ResNet-12 network pre-trained with *miniImageNet*. Unlike domain-shared prompts, this method is equivalent to introducing some prior knowledge of the current data, thus enhancing the feature extraction capability of the model. The fourth line is the effect of our combination of domain-shared and task-specific prompts, showing that the two prompts can complement each other and greatly improve the performance of the model.

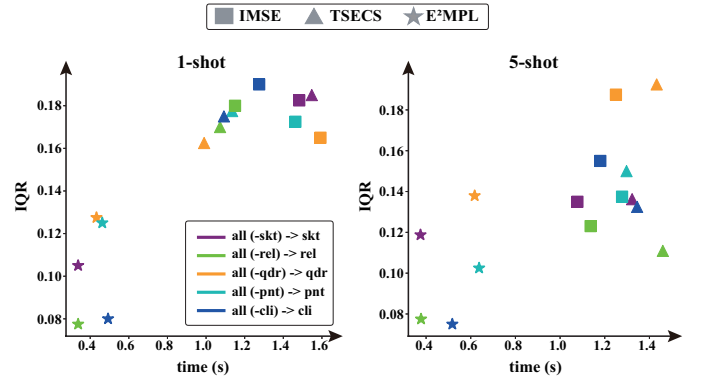


Fig. 3: Comparison of the average adaptation time (seconds) each task and classification accuracy (boxplot IQR value) for 3600 test tasks. The proposed E²MPL has lower time cost and a lower IQR value for both 5-way 1-shot and 5-way 5-shot training settings.

TABLE V: The effect of domain generalization in our E²MPL: the averaged classification accuracy (%) and variance over 3600 tasks on *DomainNet* for backbone CLIP. The higher accuracy and less variance value are shown in bold.

meta-train	skt \Rightarrow rel	skt \Rightarrow rel	skt \Rightarrow rel	pnt \Rightarrow cli	pnt \Rightarrow cli	pnt \Rightarrow cli	qdr \Rightarrow pnt	qdr \Rightarrow pnt	qdr \Rightarrow pnt
meta-test	skt \Rightarrow qdr	skt \Rightarrow pnt	skt \Rightarrow cli	pnt \Rightarrow skt	pnt \Rightarrow rel	pnt \Rightarrow qdr	qdr \Rightarrow skt	qdr \Rightarrow rel	qdr \Rightarrow cli
5-way, 1-shot (acc/var)									
IMSE	59.91/0.014	80.14/0.015	87.31/0.017	55.39/0.018	80.26/0.019	88.75/0.017	69.12/0.019	76.27/0.015	73.64/0.018
TSECS	66.75/0.011	86.15/0.014	92.27/0.011	62.85/0.014	85.63/0.015	92.76/0.012	74.53/0.016	80.76/0.011	80.71/0.012
E ² MPL	72.54/0.009	87.20/0.012	93.77/0.009	69.97/0.012	88.31/0.013	93.31/0.009	79.96/0.015	84.19/0.009	83.42/0.003
5-way, 5-shot (acc/var)									
IMSE	63.81/0.013	82.36/0.010	89.62/0.011	61.25/0.018	82.86/0.011	87.93/0.012	71.10/0.013	78.73/0.006	76.82/0.014
TSECS	67.37/0.012	88.24/0.008	93.25/0.006	65.19/0.010	89.17/0.007	94.94/0.011	78.34/0.010	84.89/0.005	83.21/0.011
E ² MPL	75.14/0.011	89.53/0.005	94.58/0.001	78.59/0.004	92.81/0.002	96.83/0.011	83.89/0.008	88.52/0.003	87.64/0.007

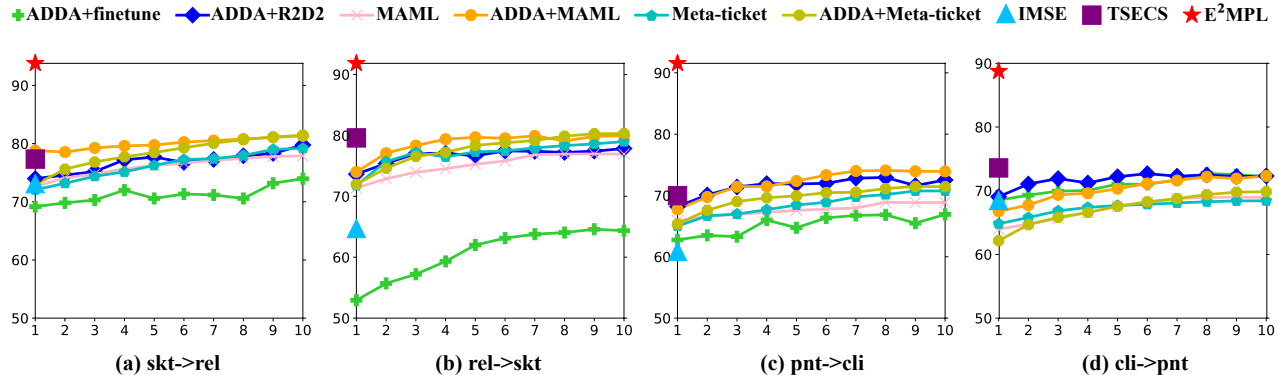


Fig. 4: Comparison of different methods for adapting to 3600 new 5-way 1-shot UDA tasks. Our E²MPL is denoted as a red star and a green square respectively.

D. Evaluation of Model Adaptation

Evaluation of adaptation time and stability to new tasks.

To validate the enduring and efficient performance of our method in new FS-UDA tasks, we evaluated the average time of model adaptation to each task, as well as the IQR value of the classification accuracy boxplot for 3600 test tasks, among the three FS-UDA methods (E²MPL, IMSE, and TSECS). Their time cost (in seconds) and accuracy IQR values are depicted in **Fig. 3**, where CLIP is the feature embedding backbone we used. Clearly, our E²MPL using bilevel optimization meta-prompt learning takes much less time and lower IQR values than IMSE and TSECS. This validates the efficiency and stability of our meta-prompt learning framework to address FS-UDA.

Model adaptation to new tasks. To further show the performance of our method to adapt to new tasks by one-step update, we compare it with the eight baselines using meta-learning for adaptation (ADDA+finetune, ADDA+R2D2, MAML, ADDA+MAML, Meta-ticket, ADDA+Meta-ticket, IMSE, and TSECS), using the CLIP backbone network for all models. The first six methods are based on meta-learning following the setting in [43], and allow 10 gradient updates to adapt to new tasks, while the latter two methods are metric-based, classifying by directly measuring sample similarities with the support set without relying on the gradient optimization process. Thus, **Fig. 4** shows the nine methods in terms of the accuracy of one-step update or accuracy changing curves under multiple gradient updates. It is evident that the inclusion of the prompt module enables E²MPL to

outperform traditional methods that combine FSL and UDA. Additionally, although IMSE and TSECS have demonstrated strong capabilities, their performance remains significantly lower than E²MPL because our model designs a lightweight but effective meta prompt learning framework.

Domain Generalization. To thoroughly understand the impact and reliability of the prompt module in domain generalization, we investigated the performance of model adaptation to a new target domain, which the model had not encountered during meta-training. We evaluated the averaged accuracy and variance values in 3600 new test tasks using CLIP as the backbone for 5-way 1-shot and 5-shot UDA tasks, shown in **Table V**. It is evidently shown that our E²MPL, with its designed meta-prompt learning, has better advantages in domain generalization and exhibits greater stability across different tasks.

E. More Results

Ablation study of three loss terms. To better demonstrate our method, we investigate the impact of the three losses in Eqn. (6). The resulting classification accuracies are shown in **Table VI**. The **all (-skt) \Rightarrow skt** means the same as above. The first line $\mathcal{L}_c^{\text{meta}}$ means that the model tries to adapt to categories without considering domain adaptation. The second line $\mathcal{L}_d^{\text{meta}}$ means that the model tries to transfer from the source domain to the target domain without considering classification generalization. $\mathcal{L}_f^{\text{meta}}$ means that only the semantic discriminative features of the classes are considered. Comparison of these three lines with the last line (*i.e.*, our E²MPL) indicates that

TABLE VI: Ablation study of the effect of the three losses in our E²MPL (backbone CLIP), where **all (-skt) \Rightarrow skt** indicates the average accuracy when other domains except for *sketch* are the source domain and *sketch* is the target domain.

$\mathcal{L}_c^{\text{meta}}$	$\mathcal{L}_d^{\text{meta}}$	$\mathcal{L}_f^{\text{meta}}$	all(-skt) \Rightarrow skt		all(-rel) \Rightarrow rel		all(-qdr) \Rightarrow qdr		all(-pnt) \Rightarrow pnt		all(-cli) \Rightarrow cli	
			1-shot	5-shot	1-shot	5-shot	1-shot	5-shot	1-shot	5-shot	1-shot	5-shot
✓			83.58	88.29	86.83	93.55	71.34	76.20	79.71	84.27	86.73	91.69
	✓		82.63	86.59	87.45	91.26	69.10	75.35	79.30	82.55	85.41	89.64
		✓	67.16	71.54	73.86	76.15	56.10	63.21	65.41	70.27	71.70	74.67
✓	✓		88.05	92.83	92.03	96.53	76.57	85.17	84.38	89.80	91.03	95.02
✓	✓	✓	89.07	93.29	93.26	96.89	78.49	85.31	85.60	90.03	92.60	95.69

TABLE VII: Ablation study of the effect of metric method and similarity matrix in our E²MPL (backbone CLIP)

γ_p	sinkhorn	skt \Rightarrow rel		rel \Rightarrow skt	
		1-shot	5-shot	1-shot	5-shot
Euc		89.41	94.48	88.03	89.61
	✓	92.82	95.60	90.81	91.55
	✓	91.81	95.04	90.15	92.85
		94.80	98.19	92.83	94.76
Cos		89.91	91.39	87.28	88.07
	✓	92.56	94.28	89.58	90.44
	✓	91.66	95.37	89.49	90.56
		93.56	97.73	91.94	93.16

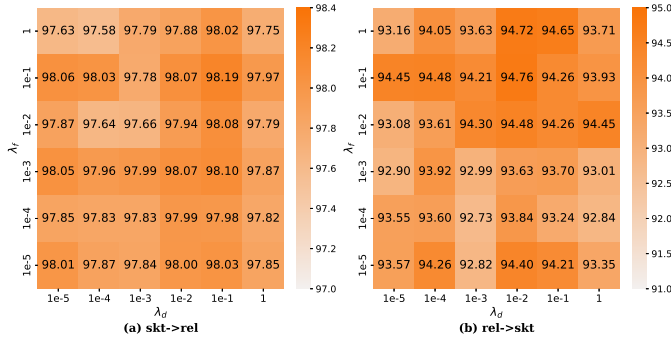


Fig. 5: The classification accuracy (%) on *DomainNet* with parameters λ_d and λ_f (backbone CLIP).

using $\mathcal{L}_c^{\text{meta}}$, $\mathcal{L}_d^{\text{meta}}$ and $\mathcal{L}_f^{\text{meta}}$ are more effective than only using one of them. This shows the necessity of E²MPL to jointly perform classification generalization and domain adaptation during meta-training for the FS-UDA setting.

Ablation study of the domain adapter. To better understand the domain adapter, we investigate the following three aspects: 1) using two different methods (Euclidean distance and Cosine similarity) to calculate the similarity matrix A in formula (11); 2) whether to use a learnable regularization coefficient γ_p ; 3) whether to regularize the similarity matrix using sinkhorn. The experimental results from *sketch* to *real* and from *real* to *sketch* are shown in **Table VII**. Obviously, the accuracy of using Euclidean distance is better than that of using Cosine similarity. Moreover, both the learnable regularization coefficients and adjacency matrix regularization can improve the performance of the domain adapter.

Effect of parameters λ_d and λ_f . We evaluate the impact of parameters λ_d and λ_f in Eqn. (6) on the performance of FS-UDA with 5-way k -shot setting for *DomainNet*, shown in Fig. 5. According to Eqn. (6), λ_d and λ_f are used to balance the classification and domain adaptation, and the larger λ_d will enhance the domain adaptation of the model, while the larger

λ_f will make the learned features more discriminative. We perform a grid search of λ_d and λ_f within $\{10^{-5}, 10^{-4}, \dots, 1\}$. As can be seen in Fig. 5, when the value of λ_d is about 10^{-2} to 10^{-1} and the value of λ_f is 10^{-1} for *DomainNet*, the optimal results are obtained in the validation set.

Effect of parameter γ_p . We show the effect of different γ_p values on the model performance through line plots. γ_p represents the regularization coefficient in Eqn. (9). **Fig. 6** shows the classification accuracy, as γ_p varies within $\{10^{-2}, 10^{-1}, \dots, 10^4\}$. The optimal γ_p value is set as 10^3 for *DomainNet*. This indicates that regularization of θ_T is effective for domain adaptation.

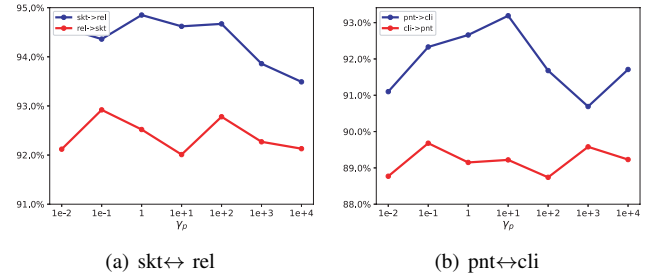


Fig. 6: The classification accuracy (%) on both datasets with varying parameter γ_p (backbone CLIP)

V. CONCLUSION

This work focuses on a realistic problem setting of FS-UDA, and for considering the stability and efficacy, we propose an enduring and efficient meta prompt learning framework (E²MPL), and design domain-shared prompts that learn domain-invariant knowledge to mitigate domain gaps, as well as task-specific prompts that generate the task-dependent prompts from pretrained prompt network to quickly adapt to new tasks. We design the bilevel optimization framework for meta-prompt learning, and leverages ridge regression and domain projection with closed-form solutions, avoiding multi-step updates in meta-training, so the meta model can be efficiently trained and adapted. Extensive experiments have confirmed the efficacy of E²MPL. In the further work, we will explore the more effective method for FS-UDA setting in real applications, *e.g.*, where the number of samples in each class may be varied.

REFERENCES

- [1] S. Huang, W. Yang, L. Wang, L. Zhou, and M. Yang, “Few-shot unsupervised domain adaptation with image-to-class sparse similarity

- encoding,” in *Proceedings of the 29th ACM International Conference on Multimedia*, ser. MM ’21. Association for Computing Machinery, 2021, p. 677–685.
- [2] W. Yang, C. Yang, S. Huang, L. Wang, and M. Yang, “Few-shot unsupervised domain adaptation via meta learning,” in *IEEE International Conference on Multimedia and Expo (ICME)*, June 2022.
 - [3] L. Yu, W. Yang, S. Huang, L. Wang, and M. Yang, “High-level semantic feature matters few-shot unsupervised domain adaptation,” in *Proceedings of the AAAI Conference on Artificial Intelligence*, vol. 37, no. 9, 2023, pp. 11 025–11 033.
 - [4] M. Jia, L. Tang, B.-C. Chen, C. Cardie, S. Belongie, B. Hariharan, and S.-N. Lim, “Visual prompt tuning,” in *European Conference on Computer Vision*, 2022.
 - [5] M. Singha, H. Pal, A. Jha, and B. Banerjee, “AD-CLIP: Adapting domains in prompt space using clip,” in *CVPR*, 2023, pp. 4255–4364.
 - [6] Q. Huang, X. Dong, D. Chen, W. Zhang, F. Wang, G. Hua, and N. Yu, “Diversity-aware meta visual prompting,” in *CVPR*, 2023, pp. 10 878–10 887.
 - [7] J. Li, M. Gao, L. Wei, S. Tang, W. Zhang, M. Li, W. Ji, Q. Tian, T.-S. Chua, and Y. Zhuang, “Gradient-regulated meta-prompt learning for generalizable vision-language models,” in *ICCV*, 2023, pp. 2551–2562.
 - [8] J. Park, J. Ko, and H. J. Kim, “Prompt learning via meta-regularization,” in *CVPR*, 2024, pp. 26 940–26 950.
 - [9] L. Franceschi, P. Frasconi, S. Salzo, R. Grazzi, and M. Pontil, “Bilevel programming for hyperparameter optimization and meta-learning,” in *International Conference on Machine Learning*, 2018.
 - [10] E. Tzeng, J. Hoffman, N. Zhang, K. Saenko, and T. Darrell, “Deep domain confusion: Maximizing for domain invariance,” *CoRR*, vol. abs/1412.3474, 2014.
 - [11] M. Long and J. Wang, “Learning transferable features with deep adaptation networks,” in *International Conference on Machine Learning*, 2015.
 - [12] K. Saito, K. Watanabe, Y. Ushiku, and T. Harada, “Maximum classifier discrepancy for unsupervised domain adaptation,” in *IEEE Conference on Computer Vision and Pattern Recognition*, 2018.
 - [13] M. Long, H. Zhu, J. Wang, and M. I. Jordan, “Unsupervised domain adaptation with residual transfer networks,” in *Advances in Neural Information Processing Systems*, 2016, pp. 136–144.
 - [14] —, “Deep transfer learning with joint adaptation networks,” in *Proceedings of the 34th International Conference on Machine Learning*, 2017, pp. 2208–2217.
 - [15] Y. Pan, T. Yao, Y. Li, Y. Wang, C.-W. Ngo, and T. Mei, “Transferable prototypical networks for unsupervised domain adaptation,” in *Proceedings of the IEEE Conference on Computer Vision and Pattern Recognition*, 2019, pp. 2239–2247.
 - [16] S. Roy, A. Siarohin, E. Sangineto, S. R. Buló, N. Sebe, and E. Ricci, “Unsupervised domain adaptation using feature-whitening and consensus loss,” in *Proceedings of the IEEE Conference on Computer Vision and Pattern Recognition*, 2019, pp. 9471–9480.
 - [17] Y. Yang, N. Jiang, Y. Xu, and D. Zhan, “Robust semi-supervised learning by wisely leveraging open-set data,” in *IEEE Transactions on Pattern Analysis and Machine Intelligence*, 2024.
 - [18] Y. Ganin and V. S. Lempitsky, “Unsupervised domain adaptation by backpropagation,” in *International Conference on Machine Learning*, 2015.
 - [19] E. Tzeng, J. Hoffman, K. Saenko, and T. Darrell, “Adversarial discriminative domain adaptation,” in *IEEE Conference on Computer Vision and Pattern Recognition*, 2017.
 - [20] C. Chen, W. Xie, W. Huang, Y. Rong, X. Ding, Y. Huang, T. Xu, and J. Huang, “Progressive feature alignment for unsupervised domain adaptation,” in *Proceedings of the IEEE Conference on Computer Vision and Pattern Recognition*, 2019, pp. 627–636.
 - [21] M. Long, Z. Cao, J. Wang, and M. I. Jordan, “Conditional adversarial domain adaptation,” in *Advances in Neural Information Processing Systems*, 2018, pp. 1640–1650.
 - [22] X. Ma, T. Zhang, and C. Xu, “GCAN: Graph convolutional adversarial network for unsupervised domain adaptation,” in *Proceedings of the IEEE Conference on Computer Vision and Pattern Recognition*, 2019, pp. 8266–8276.
 - [23] Y. Yang, H. Wei, H. Zhu, D. Yu, H. Xiong, and J. Yang, “Exploiting cross-modal prediction and relation consistency for semi-supervised image captioning,” in *IEEE Transactions on Cybernetics*, 2022.
 - [24] Y. Yang, J. Yang, R. Bao, D. Zhan, H. Zhu, X. Gao, H. Xiong, and J. Yang, “Corporate relative valuation using heterogeneous multi-modal graph neural network,” in *IEEE Transactions on Knowledge and Data Engineering*, 2022.
 - [25] Y. Yang, C. Zhang, X. Song, Z. Dong, and H. Zhu, “Contextualized knowledge graph embedding for explainable talent training course recommendation,” in *ACM Transactions on Information Systems*, 2023.
 - [26] Z. Wang, Z. Zhang, C.-Y. Lee, H. Zhang, R. Sun, X. Ren, G. Su, V. Perot, J. Dy, and T. Pfister, “Learning to prompt for continual learning,” in *CVPR*, 2022, pp. 139–149.
 - [27] A. Li, L. Zhuang, S. Fan, and S. Wang, “Learning common and specific visual prompts for domain generalization,” in *ACCV*, 2022, pp. 578–593.
 - [28] T. Ma, Y. Sun, Z. Yang, and Y. Yang, “Prod: Prompting-to-disentangle domain knowledge for cross-domain few-shot image classification,” in *CVPR*, 2023, pp. 19 754–19 763.
 - [29] H. Bahng, A. Jahanian, S. Sankaranarayanan, and P. Isola, “Visual prompting: Modifying pixel space to adapt pre-trained models,” in *arXiv*, 2022.
 - [30] J. Wu, X. Li, C. Wei, H. Wang, A. Yuille, Y. Zhou, and C. Xie, “Unleashing the power of visual prompting at the pixel level,” in *arXiv*, 2022.
 - [31] A. Chen, P. Lorenz, Y. Yao, P.-Y. Chen, and S. Liu, “Visual prompting for adversarial robustness,” in *ICASSP*, 2023.
 - [32] X. Nie, B. Ni, J. Chang, G. Meng, C. Huo, Z. Zhang, S. Xiang, Q. Tian, and C. Pan, “Pro-tuning: Unified prompt tuning for vision tasks,” in *IEEE Transactions on Circuits and Systems for Video Technology*, 2023.
 - [33] J. Loedeman, M. C. Stol, T. Han, and Y. M. Asano, “Prompt generation networks for efficient adaptation of frozen vision transformers,” in *arXiv*, 2022.
 - [34] H. Wang, J. Chang, X. Luo, J. Sun, Z. Lin, and Q. Tian, “Lion: Implicit vision prompt tuning,” in *AAAI*, 2024.
 - [35] Z. Zheng, X. Yue, K. Wang, and Y. You, “Prompt vision transformer for domain generalization,” in *arXiv*, 2022.
 - [36] Y. Zhang, K. Zhou, and Z. Liu, “Neural prompt search,” in *IEEE Transactions on Pattern Analysis and Machine Intelligence*, 2025, pp. 5268–5280.
 - [37] N. Houlsby, A. Giurugi, S. Jastrzebski, B. Morrone, Q. D. Laroussilhe, A. Gesmundo, M. Attariyan, and S. Gelly, “Parameter-efficient transfer learning for nlp,” in *Proceedings of the 36th International Conference on Machine Learning*, 2019, pp. 2790–2799.
 - [38] E. J. Hu, Y. Shen, P. Wallis, Z. Allen-Zhu, Y. Li, S. Wang, L. Wang, and W. Chen, “Lora: Low-rank adaptation of large language models,” in *Proceedings of the International Conference on Learning Representations*, 2021.
 - [39] K. Zhou, J. Yang, C. C. Loy, and Z. Liu, “Learning to prompt for vision-language models,” in *IJCV*, 2022.
 - [40] —, “Conditional prompt learning for vision-language models,” in *CVPR*, 2022.
 - [41] M. Singha, A. Jha, B. Solanki, S. Bose, and B. Banerjee, “Applenet: Visual attention parameterized prompt learning for few-shot remote sensing image generalization using clip,” in *CVPR*, 2023, pp. 2024–2034.
 - [42] S. Ravi and H. Larochelle, “Optimization as a model for few-shot learning,” in *International Conference on Learning Representations*, 2017.
 - [43] C. Finn, P. Abbeel, and S. Levine, “Model-agnostic meta-learning for fast adaptation of deep networks,” in *International Conference on Machine Learning*, 2017.
 - [44] Z. Li, F. Zhou, F. Chen, and H. Li, “Meta-SGD: Learning to learn quickly for few shot learning,” *CoRR*, vol. abs/1707.09835, 2017.
 - [45] A. A. Rusu, D. Rao, J. Sygnowski, O. Vinyals, R. Pascanu, S. Osindero, and R. Hadsell, “Meta-learning with latent embedding optimization,” in *International Conference on Learning Representations*, 2019.
 - [46] X. Qin, X. Song, and S. Jiang, “Bi-level meta-learning for few-shot domain generalization,” in *CVPR*, 2023, pp. 15 900–15 910.
 - [47] J. Snell, K. Swersky, and R. S. Zemel, “Prototypical networks for few-shot learning,” in *Neural Information Processing Systems*, 2017.
 - [48] W. Li, L. Wang, J. Xu, J. Huo, Y. Gao, and J. Luo, “Revisiting local descriptor based image-to-class measure for few-shot learning,” in *IEEE Conference on Computer Vision and Pattern Recognition*, 2019, pp. 7260–7268.
 - [49] H. Ye, H. Hu, D. Zhan, and F. Sha, “Few-shot learning via embedding adaptation with set-to-set functions,” in *CVPR*, 2020, pp. 8805–8814.
 - [50] O. Vinyals, C. Blundell, T. P. Lillicrap, K. Kavukcuoglu, and D. Wierstra, “Matching networks for one shot learning,” in *Neural Information Processing Systems*, 2016, pp. 3630–3638.
 - [51] W. Li, J. Xu, J. Huo, L. Wang, Y. Gao, and J. Luo, “Distribution consistency based covariance metric networks for few-shot learning,” in *AAAI Conference on Artificial Intelligence*, 2019.

- [52] L. Bertinetto, J. F. Henriques, P. H. Torr, and A. Vedaldi, "Meta-learning with differentiable closed-form solvers," in *International Conference on Learning Representations*, 2019.
- [53] K. B. Petersen and M. S. Pedersen, "The matrix cookbook," in *Technical University of Denmark*, 2008.
- [54] W.-H. Li, X. Liu, and H. Bilen, "Cross-domain few-shot learning with task-specific adapters," in *IEEE/CVF Conference on Computer Vision and Pattern Recognition*, 2022, pp. 7151–7160.
- [55] X. Peng, Q. Bai, X. Xia, Z. Huang, K. Saenko, and B. Wang, "Moment matching for multi-source domain adaptation," in *ICCV*, 2019, pp. 1406–1415.
- [56] A. Radford, J. W. Kim, C. Hallacy, A. Ramesh, G. Goh, S. Agarwal, G. Sastry, A. Askell, P. Mishkin, J. Clark, G. Krueger, and I. Sutskever, "Learning transferable visual models from natural language supervision," in *International Conference on Machine Learning*, 2021.
- [57] K. Lee, S. Maji, A. Ravichandran, and S. Soatto, "Meta-learning with differentiable convex optimization," in *IEEE Conference on Computer Vision and Pattern Recognition*, 2019.
- [58] Y. Yang, Y. Zhang, X. Song, and Y. Xu, "Not all out-of-distribution data are harmful to open-set active learning," in *Thirty-seventh Conference on Neural Information Processing Systems*, 2023.
- [59] Y. Yang, J. Zhang, F. Gao, X. Gao, and H. Zhu, "Domfn: A divergence-orientated multi-modal fusion network for resume assessment," in *Thirty-eighth Conference on Neural Information Processing Systems*, 2022.
- [60] Z. Fu, K. Song, L. Zhou, and Y. Yang, "Noise-aware image captioning with progressively exploring mismatched words," in *Proceedings of the 38th AAAI Conference on Artificial Intelligence*, 2024.
- [61] D. Chijiwa, S. Yamaguchi, A. Kumagai, and Y. Ida, "Meta-ticket: Finding optimal subnetworks for few-shot learning within randomly initialized neural networks," in *Annual Conference on Neural Information Processing Systems*, 2022.
- [62] W.-Y. Chen, Y.-C. Liu, Z. Kira, Y.-C. F. Wang, and J.-B. Huang, "A closer look at few-shot classification," in *International Conference on Learning Representations*, 2019.
- [63] W. Li, L. Wang, J. Huo, Y. Shi, Y. Gao, and J. Luo, "Asymmetric distribution measure for few-shot learning," in *International Joint Conference on Artificial Intelligence*, 2020, pp. 2957–2963.
- [64] C. Zhang, Y. Cai, G. Lin, and C. Shen, "Deepemd: Differentiable earth mover's distance for few-shot learning," in *IEEE Transactions on Pattern Analysis and Machine Intelligence*, 2022, pp. 5632–5648.